https://doi.org/10.5194/sp-2023-31
Preprint. Discussion started: 29 August 2023

STATE OF THE PLANET Discussions

Monitoring the record-breaking wave event in Melilla harbour (SW Mediterranean Sea)

Pablo Lorente[1], Marta De Alfonso[1], Pilar Gil[1], Fernando Manzano[1], Anna Magdalena Matulka[1], Begoña Pérez-Gómez[1], Susana Pérez-Rubio[1] and M. Isabel Ruiz[1]

[1]Puertos del Estado, Madrid, 28042, Spain

Correspondence to: Pablo Lorente (plorente@puertos.es)

Abstract. The accurate monitoring and understanding of violent weather-related hazards are decisive to adopt prevention strategies and enhance the socio-ecological resilience of coastal communities. A record-breaking wave storm hit Melilla harbour (Alborán Sea) during the 4th-5th of April 2022. The maximum significant wave height (SWH) and mean period registered by a coastal buoy were 7.32 m and 9.42 s, respectively, beating previous historical records. Port decision-makers precautionary suspended maritime operations for security reasons due to the prevailing harsh weather, the overtopping of breakwaters and the presence of extreme harbour agitation (1.41 m) and sea level oscillations dominated by the infragravity band. In this work, the record-breaking event was analysed and retrospectively compared against six previous extreme wave episodes. All of them were connected with similar large-scale atmospheric driving forces: a dipole-like sea level pressure (SLP) pattern, characterised by two adjacent (northern) high and (southern) low pressure systems, which induced strong easterly winds over the entire Alborán Sea. The 2022 record-breaking event differed from the rest in the much stronger SLP gradient (2 $Pa \cdot km^{-1}$). The common atmospheric configuration seems to predominantly feature during the same stage of the year, a 6-week period between late February and early April, contrasting with NW Spanish harbours where the storm season typically spans from November to March. Finally, a 30-year (1993-2022) regional wave reanalysis product was used to characterise the intra-annual variability of the 99th percentile (P99) of SWH along the Alborán Sea and identify the existence of trends. Results revealed that the intensity of extreme wave events impacting Melilla harbour have increased for April while observed trends indicate a significant decrease of the P99 of SWH for June and October.

1 Introduction

Over recent decades, climate change and extreme weather events have attracted growing public concern and political attention due to its widespread impact on the environment and human wellbeing (Konisky et al., 2015). While the global ocean is already experiencing anthropogenic-driven variations such as gradual warming, acidification, and sea level rise (IPCC, 2022), sustained pressure from climate change is even more significant on semi-enclosed basins like the Mediterranean Sea due to its singular geomorphology (Chiggiato et al., 2023; Juza and Tintoré, 2021).

https://doi.org/10.5194/sp-2023-31
Preprint. Discussion started: 29 August 2023

The Mediterranean Sea has long been recognized as a vulnerable climate change hot spot (Tuel and Eltahir, 2020), seriously jeopardised by marine pollution episodes or litter accumulation (Soussi et al., 2020; Ramirez-Llodra et al., 2013). This region is often affected by marine heat waves, mass mortality events and violent hazards, ranging from storm surges and flash floods to rogue waves and Medicanes (Dayan et al., 2023; Garrabou et al., 2022; Milglietta and Rotunno, 2019; Wolff et al., 2018; Cavaleri et al., 2012). Served as examples, the 2018 Medicane Zorbas or the 2020 storm Gloria resulted in casualties and multi-million damages in susceptible coastal areas (Álvarez-Fanjul et al., 2022; Scicchitano et al., 2021; Lorente et al., 2021; Sotillo et al., 2021; Pérez-Gómez et al., 2021).

Consequently, there is an increasing awareness not only about the potential anthropogenic influence on the intensity of these extreme weather episodes but also about the unavoidable need of gaining insight into the underlying physical processes (Eyring et al., 2021). Their comprehensive monitoring is crucial to implement adaptation policies, adopt prevention strategies, reduce coastal vulnerability, and mitigate the destructive effects in human infrastructures and related services (Izaguirre et al., 2021; Linnenluecke et al., 2012). In response to this requisite, successive editions of the Copernicus Ocean State Report initiative have traditionally placed special emphasis on the multi-parameter analysis of severe sea states (Table 2).

Recent initiatives like ECCLIPSE (assEssment of CLImate change in Ports of Southwest Europe) Interreg Sudoe project (ECCLIPSE website) have focused on analysing the impact of climate change on seaports. Although this topic has historically received less consideration than the corresponding impact for beach systems (Sánchez-Arcilla et al., 2016a and 2016b), the central role of ports in countries' growth and globalised economy have motivated a plethora of newborn studies in the Mediterranean Sea (Portillo Juan et al., 2022; Sierra et al., 2015 and 2017). In this sense, one of the main objectives of this project was to establish the fundamentals of a climate change observatory for Spanish ports, aiming at monitoring essential ocean variables and gaining an holistic understanding of extreme weather from its physical drivers to its impact on port operability and infrastructure (Table 3).

Following the footprints of ECCLIPSE, this work attempts to characterise the record-breaking storm that hit the Alborán Sea (south-western Mediterranean Sea, Figure 1-a) with waves above 7 m during the 4th-5th of April 2022 and evaluate the energetic response of Melilla harbour basins (Figure 1, b-c) under the penetrating wave action. Port operations were precautionary disrupted due to the prevailing harsh weather conditions, the overtopping of breakwaters and the presence of record harbour agitation and infragravity (IG) waves with periods between 25-30 s and 300-600 s (Bellafont, 2019; Elgar et al., 1992). While one ship was evacuated from its berth and later sheltered at the lee of Ras Taksefi Cape (Figure 1, b), structural damages were reported in the seawall tip and in several boats and marina pontoons.

Within this context, it is noteworthy that the Melilla area is usually dominated by a low energy wave climate with mean significant wave heights (SWH) below 0.7 m (Table 4), in contrast to other western Mediterranean Sea regions like the Gulf of Lion (Figure 1, a) where highly energetic waves (above 5 m) can be frequently observed during wintertime (Guizien, 2009). Therefore, a retrospective comparison of the present study case against six previous extreme events (with SWH values above the 99.9th percentile, denoted in Figure 1-d) was conducted not only to put the former into a broader historical

https://doi.org/10.5194/sp-2023-31
Preprint. Discussion started: 29 August 2023

context but also to disentangle their common driving mechanisms (i.e., the predominant atmospheric conditions at synoptic scale).

Additionally, following the approach of Pérez-Gómez et al. (2021) for 2020 storm Gloria, high frequency (2 Hz) sea level data and agitation observations provided by Melilla tide-gauge (Figure 1, b-c) were used to investigate the relationship between offshore energetic conditions and the sea state inside of the harbour (including the IG energy band). The monitoring of IG waves is a red-hot issue since their presence in semi-closed ports of small to intermediate size (where the surface water area and depth are about 1-10 km^2 and 5-10 m, respectively) may cause excessive ship motions and unacceptable forces on mooring lines, among other problematic effects (Costas et al., 2022; Bellotti and Franco, 2011). Under adverse circumstances, IG waves can be highly amplified by the basin geometry due to resonant processes (commonly referred to as seiches), resulting in large water level fluctuations and strong horizontal currents within the harbour that disturb port operations and negatively impact on cost-time efficiency (López and Iglesias, 2014; Okihiro et al., 1993), as reflected in Table 3.

Finally, a regional wave reanalysis product developed in the frame of the Copernicus Marine Service for the Mediterranean Sea was analysed to: i) infer its accuracy in the study-area and thereby the historical occurrence of similar extreme episodes; ii) characterise the spatial variability of the long-term extreme value wave climate along the Alborán Sea. The intra-annual variability of the 99th percentile (P99) of SWH was examined at monthly timescale to identify potential trends, thereby complementing similar studies previously focused on the intra-seasonal (Barbariol el al., 2021) or the inter-annual (Zacharioudaki et al., 2022b; Morales-Márquez et al., 2020) climate variability of extreme waves in the entire Mediterranean basin.

This work is structured as follows: Section 2 outlines the observational and modelled data sources. Section 3 describes the methodology adopted. Results are presented and discussed in Section 4. Finally, principal conclusions are drawn in Section 5.

2 Data

All the observational and modelled products used in this study are gathered in Table 1 and briefly described below.

2.1 ERA5 reanalysis

ERA5 is the fifth-generation reanalysis for the global climate and weather generated by the European Centre for Medium-Range Weather Forecast. Data is available from 1940 onwards (product ref. no. 1 in Table 1). ERA5 provides hourly estimates for a large number of atmospheric parameters (among other quantities) which are regridded to a 0.25° regular grid. In this work, hourly maps of sea level pressure (SLP) and wind at 10 m height were analysed at synoptic scale.

https://doi.org/10.5194/sp-2023-31
Preprint. Discussion started: 29 August 2023

2.2 Wave forecast model

Puertos del Estado and the Spanish Meteorological Agency run twice a day a WAM-based wave forecast system (product ref. no. 2 in Table 1), providing hourly wave outputs with a 72-h forecast horizon. In this work, hourly maps of SWH were used to examine the fingerprint of the wave storm during the 4th of April 2022 (Figure 1, a-b).

2.3 Tide-gauge

A radar tide-gauge, manufactured by Miros and operated by Puertos del Estado as part of its REDMAR network (Pérez-Gómez et al., 2008), was deployed inside of Melilla harbour in October 2007 (Figure 1, b-c). Since it provides quality-controlled high frequency (2 Hz) sea level data (product ref. no. 3 in Table 1), immediate evaluation of specific physical phenomena contained in raw data (such as meteotsunamis and IG waves) can be achieved (García-Valdecasas et al., 2021). Furthermore, 20-minute averaged estimations of agitation (i.e., oscillations within the port due to wind waves) were examined for the period 2015-2022 to assess the impact of the wave storm.

2.4 In situ coastal buoy

A Datawell scalar buoy was moored at 15 m depth in April 2008, close to Melilla harbour (Figure 1, b-c). Two years later, it was replaced by a Triaxys buoy able to provide directional information. This in situ device, operated by Puertos del Estado, collects quality-controlled hourly estimations of sea surface temperature and diverse wave parameters (product ref. no. 4 in Table 1).

2.5 Multi-year wave product

The multi-year wave product of the Mediterranean Sea Waves forecasting system (product ref. no. 5 in Table 1) is based on the WAM model and contains a reanalysis dataset (from January 1993) and an interim dataset covering the period after the reanalysis until one month before present. The dataset is composed of hourly wave parameters at 1/24° horizontal resolution. In the present work, hourly SWH estimations over the entire Alborán Sea (Figure 1, a) were analysed for the period 1993-2022.

3 Methodology

As not all extreme metocean hazards necessarily have destructive impacts on coastal areas, there is not a worldwide consensus on the protocol for their categorization. A weather-related event is generally defined as extreme when a single or several interconnected variables persistently exceed specific thresholds, which can be determined according to percentile-based values, fixed absolute values or return periods (Radovic and Iglesias, 2018).

https://doi.org/10.5194/sp-2023-31
Preprint. Discussion started: 29 August 2023

In the present work, we firstly used the percentile method, which defines extreme events as the occurrence of values higher than the reference P99 threshold for a certain number of hours. P99 values, along with P50, P90 and P99.9 values, were computed on the whole time series (2008-2022) of diverse wave parameters registered by Melilla coastal buoy in order to comprehensively characterise the wave climate Melilla area (Table 4) and categorise seven extreme wave events. Complementarily, the return period associated with those extreme episodes was calculated. The notion of return period, which is defined as the average time interval between two consecutive events exceeding a specific SWH value, is often used in marine engineering for the design of port facilities and the identification of dangerous events, providing a means for rational decision making and risk assessment (Salvadori et al., 2013). For instance, harbour breakwaters are commonly designed to withstand 100-year return period metocean conditions without significant damage, while having service lifetimes of similar durations (Todd et al., 2012; Gutierrez-Serret et al., 2009). In this work, the analysis was conducted using the time series of SWH for two different periods: a) 2010-2020 (before the record-breaking storm) and (b) 2010-2022 (including the storm). The long-term extreme sea state was characterised by using the Peak over Threshold (POT) method (Goda, 1998) with the fitting of a Three-Parameter Weibull probability distribution to the SWH observations. The POT method is based on extracting, from the recorded time series, those individual storms which are not dependant upon another one due to their proximity in time, and that surpass the exceedance threshold of SWH (established for each region in function of its own wave climate, see Table 5) in the peak of the storm. The 3-parameter Weibull distribution was computed following the approach proposed by De Alfonso et al. (2021) to obtain the return period for the maximum SWH registered during the seven selected events (Table 5).

In situ data time series were processed as follows: spikes or spurious values were discarded, and occasional gaps were linearly interpolated to ensure the continuity of the records. The statistical metrics used in the present study to compare two data sets $x = \{x_1, x_2, x_3 \dots x_N\}$ and $y = \{y_1, y_2, y_3 \dots y_N\}$ (where 1, 2, … N represent the time steps) include the mean, the standard deviation, and the correlation coefficient, defined respectively as:

$$\bar{x} = \frac{1}{N}\sum_{i=1}^{N} x_i \quad (1)$$

$$\sigma = \sqrt{\frac{1}{N-1}\sum_{i=1}^{N}(x_i - \bar{x})^2} \quad (2)$$

$$\text{Correlation} = \frac{1}{N-1}\sum_{i=1}^{N}\left(\frac{x_i-\bar{x}}{\sigma_x}\right)\left(\frac{y_i-\bar{y}}{\sigma_y}\right) \quad (3)$$

where σ_x and σ_y are the standard deviation of x and y, respectively.

The relationship between energetic offshore conditions and agitation and IG waves maximum height inside the harbour (IG_{max}) was investigated. The spectra of 2 Hz sea level oscillations measured by the tide gauge revealed a high energy content in the IG band during the seven storms, reaching a record value during the E7 event. As the IG energy in the nearshore has been documented to be positively correlated with offshore SWH (Inch et al., 2017; Stockdon et al., 2006), a

https://doi.org/10.5194/sp-2023-31
Preprint. Discussion started: 29 August 2023

scatter plot was computed to disentangle which peak periods could yield severe IG waves within the port. Furthermore, the high frequency (30 s – 1 h) sea level oscillations heights recorded within Melilla harbour during the seven storms were categorized based on specific thresholds (Table 6) which are universally common to all locations (McComb et al., 2020; McComb, 2011).

Equally, the connection between harbour agitation and the wave field (SWH, period and incoming direction) outside the port was investigated through the computation of a scatterplot, assuming the following relationship (Inch et al., 2017):

$$\text{Agitation} \sim \sqrt{\text{SWH} \cdot \text{L}} \tag{4}$$

The deep-water wavelength (L) is defined as follows:

$$\text{L} = \frac{\text{g} \cdot \text{T}^2}{2\pi} \tag{5}$$

where the gravity acceleration g is 9.8 $m \cdot s^{-2}$ and T is the wave period in seconds, respectively.

Finally, potential long-term changes in the extreme sea state climate during the 30-year period analysed (1993-2022) were assessed through the estimation of maps of linear trend for the SWH over the entire Alborán Seas at monthly timescales. The attention was particularly focused on the intra-annual variability in order to complement prior research dealing with intra-seasonal and inter-annual variability of extreme waves in the entire Mediterranean basin. (Barbariol el al., 2021; Zacharioudaki et al., 2022b; Morales-Márquez et al., 2020). The presence of temporal tendencies in the SWH reanalysis time series was evaluated with two well-known non-parametric tests:

i) trends were calculated using the Sen´s slope estimator of P99 because it is not subject to the influence of extreme values (outliers) and therefore is more consistent than simple linear regression methods (Sen, 1968).

ii) the statistical significance at the 90% confidence interval was assessed with the Mann-Kendall test (Mann, 1945; Kendall, 1962), in accordance with similar works previously published (Caloiero and Aristodemo, 2021; Barbariol et. al, 2021).

4 Results

4.1 Extreme events analysis

The unprecedented storm that hit Melilla harbour during the 4th-5th of April 2022 clearly beat historical records of SWH in terms of intensity and duration. The P99, set to 2.92 m (Table 4) and derived from a long-term time series provided by a Melilla coastal buoy (Figure 1, b-c), was abruptly exceeded during 42 consecutive hours. The peak of SWH (7.32 m), coincident with a maximum value of mean wave period (9.42 s), beat previous historical records. Additionally, a retrospective comparison of the record-breaking storm against the six most extreme events previously occurred in Melilla was performed to put the former into a broader historical context. The seven episodes were tagged in chronological order, as shown in Figure 1d. All of them exhibited SWH values fairly above the P99.9 of SWH (4.44 m, Table 4) and above the P99 of mean period (6.29 s, Table 4). From a directional perspective (Figure 1, f), the prevailing incoming wave directions during the 12-year period 2011-2022 were NE and NE-E (58 ± 37)º. These are the most common origins for waves recorded at

https://doi.org/10.5194/sp-2023-31
Preprint. Discussion started: 29 August 2023

Melilla coastal buoy due to its particular emplacement, sheltered to the east of Ras Taksefi Cape (Figure 1, b). As a result, the shadow effect of this coastal promontory prevents the angular spreading of the storms coming from the westernmost sector.

4.2 Return period analysis

The analysis was conducted using hourly time series of SWH from Melilla coastal buoy for two different periods, assuming an exceedance threshold of 2 m (previously derived from the wave climate in the study area) and 5 days distance between two independent stormy events (Table 5). For the period 2010-2020, the entire time series was fitted to a 3-parameter Weibull distribution, leading to return periods of 3.5-4.5 years for the extreme wave events E1 to E6. Notwithstanding, the E7 event was associated with a 45-y return period which highlights the extraordinary magnitude of this twice-in-a-century high-impact episode.

For the period 2010-2022, which already included not only the E6 event (March 2021) but also the record-breaking E7 storm (April 2022), a new fitting of the 3-parameter Weibull probability distribution to the SWH observations was performed (Table 5). Results revealed that the return period related to E1 to E6 events decreased by 20-24% to 2.5-3.5 years, while the updated E7 return period dropped 45% (25 years). These relevant outcomes should be applicable in the design and construction of new facilities at Melilla harbour and also integrated into the port operations planning and day-to-day logistics activities.

4.3 Driving atmospheric conditions

The prevailing atmospheric conditions at synoptic scale during the wave storm were inferred from the ERA5 reanalysis of SLP and wind at 10 m height. The SLP pattern was characterised by two adjacent (north-western) high and (southern) low pressure systems (Figure 2, a). This persistent dipole was visible for the whole investigation period, whereas it followed a clockwise rotation. The derived pressure gradient (above 2 $Pa \cdot km^{-1}$) gave rise to very strong north-easterly winds (above 20 $m \cdot s^{-1}$) that affected broad areas of the SW Mediterranean and Alborán Seas, while extremely intense easterlies were channelled through the Strait of Gibraltar due to its specific geometric configuration (Figure 2, b). In the Gulf of Cádiz, the wind field exhibited a counterclockwise rotation around the low-pressure core.

The analyses of the six previous extreme events (listed in Figure 1d) revealed that all of them shared very similar meteorological conditions: i) a north-south dipole-like pattern of SLP anomalies (Annex 1), in contrast to the climatological mean (Figure 2, c) that shows two well-known semi-permanent pressure systems (i.e., the Azores High at middle latitudes and the Icelandic Low at subpolar latitudes); ii) a peak of wind speed over the entire Alborán Sea, where easterlies blew persistently along both sides of the Strait of Gibraltar (Annex 2). Only the event E6 showed a slightly different structure (Annex 2, f), with moderately strong winds blowing from the NE and only affecting the NW Mediterranean Sea.

Furthermore, it should be noted that the seven extreme episodes took place during the same stage of the year, a 6-week period between late February and early April (Figure 1, d). Therefore, it might be deduced that the large-scale atmospheric

https://doi.org/10.5194/sp-2023-31
Preprint. Discussion started: 29 August 2023

configuration leading to severe sea states in Melilla apparently tend to be more probable during the winter-to-spring transition period.

The primary factor that triggered the record-breaking wave storm (E7 event) was the short distance (1400 km) between the two main pressure systems, rather than the associated SLP values (Figure 2, a-b). The resulting SLP gradient was anomalously powerful (above 2 $Pa \cdot km^{-1}$), leading to very strong, persistent easterlies that ultimately induced high waves over the entire Alborán Sea. The P99 of SWH, set to 2.92 m (Table 4) and derived from long-term time series provided by Melilla coastal buoy (Figure 1, b-c), was abruptly exceeded during 42 consecutive hours (Figure 1, d). The previous six episodes also presented intense (albeit weaker) SLP gradients, ranging from 1.01 $Pa \cdot km^{-1}$ (event E4, Annex 1d) to 1.48 $Pa \cdot km^{-1}$ (event E6, Annex 1f), due to the usually longer distances (ranging from 1900 km to 3000 km) comprised between both pressure systems (Annex 1). Although the E1 event exhibited SLP cores with similar separation (1438 km, showed in Annex 1a), the low-pressure system was not deep (1016 hPa), in contrast to the E7 event where minimum SLP values dropped below 1000 hPa (Figure 2, a).

4.4 Sea state within the port

Here we focus on the most common type of IG waves, those induced by the non-linear interactions between incident wind short waves (Belloti and Franco, 2011). While IG waves tend to go unnoticed to human perception in deep waters (heights of the order of few cm), they can abruptly increase near the coastline and even exceed 1 m (Aucan and Ardhuin, 2013), contributing significantly to nearshore processes (beach erosion) and affecting coastal structures (Okihiro et al. 1993).

The hourly timeseries of maximum sea level oscillations heights (30 s – 1 h) showed that the seven extreme episodes surpassed the P99 (0.28 m) threshold, while only four of them -E3, E4, E5 and E7- exceeded also the P99.9 (0.44 m) threshold (Figure 3, a). According to the spectra content of 2 Hz data, these oscillations are highly dominated by the IG band energy during the analysed events.

Operational thresholds in the IG band, which are common to all locations, have been historically proposed for safe conditions during port operations (McComb et al., 2020; McComb, 2011). According to Table 6, hourly records of sea level oscillations (30 s – 1 h) height for the seven extreme events (not shown) were beyond the limit of 0.2 m, except for E6 case where values ranged from 0.047 to 0.194 m. The maximum height values were clearly above that limit, with an unprecedented value of 0.58 m during the E7 episode.

The scatter plot showed a strong correlation (0.8) between the offshore incident SWH and the energy in the IG band inside the port (Figure 3, b). As expected, the highest IG energy was observed for energetic swell waves (with SWH and peak period above 5 m and 10 s, respectively).

An accurate estimation of the historical harbour wave agitation is fundamental for many practical applications such as port downtime analysis (Romano-Moreno et al., 2022). The analysis of 20-m timeseries of agitation provided by Melilla tide gauge revealed that the seven extreme events exceeded the P99 (0.38 m) threshold and only E6 did not beat the P99.9 (0.6 m) threshold (Figure 3, c). In particular, during E7 event there was a record-breaking value of agitation (1.4 m), a 233%

https://doi.org/10.5194/sp-2023-31
Preprint. Discussion started: 29 August 2023

higher than the P99.9 threshold. The agitation response is determined by wave penetration into the harbour arising from the combination of diverse parameters, namely: SWH, wave period and direction, astronomical tide and storm surge outside the port (Camus et al., 2018). The impact of the last two elements on harbour agitation was not taken into account since: i) the Mediterranean Sea is a microtidal environment with tidal ranges below 1 m (Samper et al., 2022); and ii) the low-pressure core was located in the western side of the Strait of Gibraltar so the storm surge affecting Melilla harbour was negligible (Figure 2, a). An hourly scatter plot evidenced the strong linear relationship between the agitation inside the port and the wave conditions outside the port registered by Melilla coastal buoy (Figure 3, d), with a significant correlation coefficient of 0.92 for an 8-year period (2015-2022). For the 655 hourly agitation values above the P99 threshold, the 90% were associated with waves coming from the predominant sector comprised between 50º and 70º (clockwise from true north), while 6% of them were related to incoming waves with angles emerging from 70º to 90º. The remaining 4% was assigned to waves with an angular spread ranging from 30º to 50º. The overall agitation is direction-dependent due to the harbour orientation (Figure 1, c) and its inherent structural design (mouth width, port layout configuration, etc.).

4.5 Trends in extreme wave climate

The evolution on the extreme wave conditions over the Alborán Sea during the 30-year period analysed (1993-2022) was assessed. As a preliminary step, a validation of the regional wave reanalysis products was conducted against hourly in situ estimations provided by Melilla coastal buoy (Figure 1, b-c) during the concurrent 14-year period 2009-2022. To this aim, the reanalysis grid point (2.916ºW, 35.354ºN) closest to the moored buoy was selected and both time series of SWH were compared. A significantly high correlation coefficient (0.95) for a set of 86925 hourly data was derived from the best linear fit of scatter plot (Annex 3, a). Equally, the slope and intercept values were close to 1 (0.85) and moderately low (0.15), respectively.

Time series of annual P99 of SWH showed a consistent qualitative agreement between the reanalysis and buoy estimations (Annex 3, b). The quantitative differences emerged in the range from 0.01 m (2009) to 0.66 m (2015), with the reanalysis systematically underestimating extreme SWH conditions. The monthly P99 values of SWH for 2009-2022 exhibited a similar visual resemblance (red and blue lines in Annex 3c), with three dominant regimes: i) a 6-month calm period (from May to October), where P99 is below 2.5 m; ii) a shorter transitional season (from November to January) with an increasing P99 usually in the range 2.5-3 m; iii) a stormy period (from February to April) with monthly P99 above 4 m (3 m) for buoy (reanalysis) estimations. It should be noted that, for both datasets, the maximum P99 is detected for April. If the entire temporal reanalysis coverage 1993-2022 is considered, slight differences can be found in the monthly P99 (green line in Annex 3c): there is a drop of P99 for April and a noticeable increase of P99 for June and October. Such changes in the intra-annual variability of the extreme wave climate in Melilla will be further discussed soon afterwards.

These results revealed that the regional wave reanalysis, albeit accurate in Melilla region, seems to underestimate wave heights, especially for extreme waves. Such systematic underestimation has been previously reported for the entire domain (Fanti et al., 2023; Zacharioudaki et al., 2022b) since shallow water processes cannot be properly captured by global and

https://doi.org/10.5194/sp-2023-31
Preprint. Discussion started: 29 August 2023

regional reanalysis because: i) the coastline and the bottom topography are not well resolved as the grid mesh is too coarse; ii) fetch limitations; iii) inherent uncertainties in the wind field used to force the wave model. These limitations are even more pronounced in regions with complex coastal configurations (sheltered by islands, headlands, and reefs) and in port-approach areas where sharp topo-bathymetric gradients pose special difficulties for accurate local predictions (Sánchez-Arcilla et al., 2016a). Nevertheless, according to Zacharioudaki et al. (2022b), the reanalysis skill can be considered robust and good enough to conduct further investigations about the wave climate and the related intra-annual variability in the Alborán Sea.

Thus, the yearly-averaged monthly P50 and P99 of SWH were computed over the entire Alborán Sea for the 1993-2022 period (Annex 4). In particular, we selected only March and July as representative months of the stormy season (peak of green line in Annex 3c) and calm period (minimum value), respectively. According to homogeneous spatial patterns of P50, the mean wave climate is rather similar for March and July, only differing in the magnitude: while March is characterised by a P50 slightly above 1.1 m over Alborán open waters in March, P50 is around 0.7-0.8 in July (Annex 4, a-b). By contrast, significant differences can be found in the most energetic sea states (Annex 4, c-d). In March, the P99 values around Melilla are up to 3 m, while they clearly exceed 4 m offshore (Annex 4, c). Peaks of 4.5 m are attained in the eastern sub-basin, probably as a consequence of strong easterly winds. On the contrary, during July the largest P99 barely reaches 3 m in the central part of Alborán Sea, while the spatial distribution of P99 generally remains uniformly below 2 m in the rest of the spatial domain, including littoral areas and nearby regions of Melilla harbour (Annex 4, d).

The climate variability over the Alborán Sea was assessed by analysing the intra-annual variations in the extreme wave conditions (Figure 4). Monthly trend maps of P99 of SWH were calculated for the period 1993-2022, revealing statistically significant changes in the vicinity of Melilla harbour for few specific months: while an increase of 2 cm·year^{-1} is observed for April (Figure 4, a), a downward P99 trend of 1.5-2 cm·year^{-1} is detected for June (Figure 4, c) and October (Figure 4, g) and, to a less extent, in July (Figure 4, e). The temporal trends for each month (Figure 4, b,d,f,h), computed over the subdomain surrounding Melilla harbour (black box in Figure 4), supported visually the previous statement. While the trends were statistically significant at the 90% confidence interval for April, June, and October, in the case of July the observed downward trend was only significant at the 80% confidence interval.

By contrast, during both the second part of summer (August - September) and the transitional season (November - February), monthly maps of P99 trends did not exhibit statistically significant values (Annex 5). Although trend maps of P99 for March (Annex 5, c) and May (Annex 5, d) showed relevant trends, they were spatially delimited to specific locations far away from Melilla harbour and the surrounding area (the scope of the present study) and therefore will not be further commented.

The long-term changes detected in the extreme wave climate over Melilla are, to a certain extent, comparable to those previously exposed by Barbariol et al. (2021). Although the wave reanalysis and its associated temporal coverage (1980-2019) were different, this previous work reported an upward trend of SWH (about 8-12 cm·decade^{-1}) in the vicinity of Melilla harbour for the extended winter (defined as NDJFM).

https://doi.org/10.5194/sp-2023-31
Preprint. Discussion started: 29 August 2023

5 Conclusions

Gaining a deeper, holistic understanding of extreme weather events and the related driving mechanisms has been identified as one of the World Climate Research Program's Grand Challenges (WCRP website) due to its detrimental impact on ecosystems health and societal assets (Hochman et al., 2022). Concerning the latter, climate-driven extreme coastal hazards have been long recognized to impose heavy socio-economic tolls, particularly aggravated in vulnerable semi-enclosed regions like the Mediterranean Sea and in exposed sectors like harbour systems (Verschuur et al., 2023).

As port downtime leads to reduction of safety levels and wide trade losses through maritime transport and global supply-chain networks (Verschuur et al., 2022), the accurate monitoring of violent weather-related episodes is decisive to adopt prevention strategies (i.e., wise design of safe port infrastructures) and mitigation measures that should eventually result in the enhancement of coastal communities' resilience.

In the present work, the attention is focused on the record-breaking storm that hit Melilla harbour (Alborán Sea, in the south-western Mediterranean Sea) with heavy rainfall, strong easterly winds, and extremely high waves during the 4th-5th of April 2022 (Figure 1, a). The P99 of SWH, set to 2.92 m and derived from hourly time series provided by a nearby coastal buoy (Figure 1, b-c), was abruptly exceeded during 42 consecutive hours. The maximum SWH and mean wave period registered were 7.32 m and 9.42 s, respectively, beating previous historical records (Figure 1, d-e). From a directional perspective, the prevailing incoming wave direction was the NE (Figure 1).

The long-term extreme wave distribution was characterised by using the return period and the percentile's method. The return period associated with different SWH values was calculated for two periods (2010-2020 and 2010-2022), revealing that it significantly decreased for the most extreme events (SWH above 5 m), as reflected in Table 5. In the specific case of the record-breaking E7 event, the return period (associated with a SWH around 7.32 m) decreased from 45 years to 25 years. These outcomes are essential for the safe design of future facilities at Melilla port (Naseef et al., 2019). Conversely, it is worth pointing out that the port is also subjected to a constant geometric modification (in the docks, basins, bathymetry, breakwaters, etc.) which in turn can induce additional variations in the port response to extreme wave events that should be further assessed.

With regards to the percentile's method, the P99.9 was applied as a threshold to the long-term time series of SWH (2008-2022) in order to categorise seven extreme wave events (Figure 1, d). The retrospective comparison of the record-breaking E7 event against six previous extreme wave episodes (E1 to E6) revealed that all of them were connected with similar large-scale atmospheric driving forces: a dipole-like SLP pattern, characterised by two adjacent (northern) high and (southern) low pressure systems, induced strong easterly winds channelled over the entire Alborán Sea (Figure 2, Annex 1 and Annex 2). Furthermore, this common atmospheric configuration seems to predominantly feature during the same stage of the year, a 6-week period between late February and early April (Figure 1, d). These findings contrast with other Spanish harbours (i.e., NW Iberian Peninsula) where the storm season typically spans from November to March (Ribeiro et al., 2023), highlighting the strong need of conducting a tailored assessment for each specific port and oceanographic region.

https://doi.org/10.5194/sp-2023-31
Preprint. Discussion started: 29 August 2023

Long-term observations of high frequency (2 Hz) sea level and agitation, provided by Melilla tide gauge, were used to investigate the relationship between offshore energetic waves and the sea state inside of the harbour (Figure 3). A record-breaking value of harbour agitation (1.4 m), a 233% higher than P99.9, was recorded during the E7 event (Figure 3, c). Extreme sea level oscillations (30 s -1 h), which also reached record heights (up to 0.58 m), were linked to the highest values in the IG energy band since the beginning of measurements (Figure 3, a). The seven extreme events in the Alborán Sea led to harsh sea conditions within the port: the energy in the IG band was significantly correlated (0.8) with the SWH and peak periods recorded by the costal buoy, with energetic swell being responsible for the highest energies (Figure 3, b). Therefore, the IG waves related to energetic swell commonly observed in the NW Iberian coast, can also be present during extreme wave events in the Mediterranean coast, as previously reported for the 2020 storm Gloria by Pérez-Gómez et al. (2021) and Álvarez-Fanjul et al. (2022). Equally, the highest agitation records were registered for incident high waves coming predominantly from the sector comprised between 50º and 70º (clockwise from true north), as shown in Figure 3d.

Additionally, a regional wave reanalysis product was used to characterise the long-term mean (Annex 4) and extreme (Figure 4 and Annex 5) wave climate over the Alborán Sea for the period 1993-2022. The intra-annual variability of the P99 of SWH was examined at monthly timescale to identify the existence of potential trends. Results seem to suggest that the intensity of extreme wave events impacting Melilla harbour has increased for April (Figure 4, a-b), while observed trends indicate a significant decrease of P99 for the SWH during June (Figure 4, c-d) or October (Figure 4, g-h). Such alterations of outer-harbour wave climate conditions might impact on in-port wave agitation response as the amount of energy penetrating into the harbour would be different, as previously indicated by Sierra et al. (2015).

Still, it should be noted that the present work does not focus on the duration of extreme wave events over the SW Mediterranean Sea, so future endeavours should address this relevant aspect to complement the results here presented. Equally, long-term historical changes in wave period and directionality are receiving increasing attention and should be further analysed to assess their specific impact on harbours operability (Erikson et al., 2022; Casas-Prat and Sierra, 2012). Permanent modifications in the wave direction might result in enhanced wave penetration into the harbour and thereby larger agitation as port protective structures were originally designed to dampen wind and short waves coming from a predetermined sector (Casas-Prat and Sierra, 2012).

Regardless of the reported limitations of global and regional reanalyses (inherent to their coarse spatial resolution) when used at coastal and port scales (Fanti et al., 2023; Zacharioudaki et al., 2022b), the wave reanalysis used in this work can be considered a robust first-guess estimator for the present intra-annual variability assessment of extreme waves in Melilla. This statement is supported not only by the comprehensive Quality Information Document (Zacharioudaki et al., 2022a) but also by the 12-year skill assessment conducted against in situ hourly observations from Melilla coastal buoy (Annex 3). The comparison yielded a correlation coefficient of 0.95 and revealed a slight underestimation of extreme SWH values. To overcome such a drawback, future works should include the implementation of a dynamical downscaling methodology to improve the wave reanalysis accuracy at finer coastal scales (Vannucchi et al., 2021). Of course, this would necessarily require finding the right trade-off between adequate spatial resolutions and the available in-house computational resources.

https://doi.org/10.5194/sp-2023-31
Preprint. Discussion started: 29 August 2023

Finally, it is worth mentioning that most of the outcomes derived from the present work could not only feed the incoming climate change observatory for the Spanish ports (which should be fully operational by 2025) but also be integrated into tailored multi-hazard early warning systems. They would act as a key component of robust capacity analysis frameworks, covering a wide range of dimensions, such as legislative, planning, infrastructure, technical, scientific and institutional partnerships (Haigh et al., 2018). Within this context, future maritime facilities at Melilla harbour should be wisely designed and constructed taking into account these outcomes in order to withstand extreme wave regimes imposed by the changing marine environment (Vanem et al., 2019).

Data availability

The model and observation products used in this study from both the Copernicus Marine Service and other sources are listed in Table 1.

Author contributions

PL, MA, PG, FM, AMM, BPG, SPR and MIR conducted the pilot study through fruitful discussions in the framework of working team meetings. PL: designed the experiment, analysed the long-term wave trends, created the figures, and prepared a first version of the draft with inputs from all co-authors. MA: conducted a bibliographic revision of extreme metocean events previously occurred in the Mediterranean Sea. PG: computed the return period before and after the record-breaking event. FM: extracted timeseries from Puertos del Estado internal database and prepared diverse in situ sensors datasets. AMM: downloaded and post-processed the reanalysis dataset. BPG: proposed the agitation and infragravity band study in the port, and analysed the corresponding tide-gauge records. SPR: provided a tailored coastline for Melilla harbour and analysed the atmospheric driving mechanisms during the event. MIR: applied a quality control for historical timeseries of wave parameters from Melilla coastal buoy. Finally, all authors participated in successive iterations, the drafting and revision of the manuscript.

Competing interests

The contact author has declared that none of the authors has any competing interests. Disclaimer. Publisher's note: Copernicus Publications remains neutral with regard to jurisdictional claims in published maps and institutional affiliations.

Acknowledgments

The authors are grateful to the Copernicus Marine Service for the data provision.

https://doi.org/10.5194/sp-2023-31
Preprint. Discussion started: 29 August 2023

References

Álvarez-Fanjul, E., Pérez Gómez, B., de Alfonso Alonso-Muñoyerro, M., Lorente, P., García Sotillo, M., Lin-Ye, J., Aznar Lecocq, R., Ruíz Gil de la Serna, M., Pérez Rubio, S., Clementi, E., Coppini, G., García-León, M., Fernandes, M., García Valdecasas, J., García Valdecasas, J.M., Santos Muñoz, D., Luna Rico, M.Y., Mestres, M., Molina, R., Tintoré, J., Mourre, B., Masina, S., Mosso, C., Reyes, E., Santana, A.: Western Mediterranean record-breaking storm Gloria: An integrated assessment based on models and observations. J Oper Oceanogr, doi:10.1080/ 1755876X.2022.2095169, 2022.

Aucan, J. and Ardhuin, F.: Infragravity waves in the deep ocean: an upward revision. Geophysical Research Letters, 40 (13), 3435-3439, doi: 10.1002/grl.50321, 2013.

Barbariol, F., Davison, S., Falcieri, F.M.., Ferretti, R., Ricchi, A., Sclavo, M. and Benetazzo, A.: Wind Waves in the Mediterranean Sea: An ERA5 Reanalysis Wind-Based Climatology. Front. Mar. Sci., 8:760614, doi: 10.3389/fmars.2021.760614, 2021.

Bellafont, F.: Role of infragravity waves on port agitation during storm events. Civil Engineering, Université de Pau et des Pays de l'Adour. English. NNT: 2019PAUU3047. Tel-02881282, 2019.

Bellotti, G. and Franco, L.: Measurement of long waves at the harbor of Marina di Carrara, Italy. Ocean Dynamics. 61, 2051–2059, doi:10.1007/s10236-011-0468-6, 2011.

Berta, M., Corgnati, L., Magaldi, M., Griffa, A., Mantovani, C. Rubio, A. Reyes, E. and Mader, J.: Small scale ocean weather during an extreme wind event in the Ligurian Sea. Journal of Operational Oceanography (Copernicus Marine Service Ocean State Report, Issue 4), Volume: 13:sup1, 149-154, doi:10.1080/1755876X.2020.1785097, 2020.

Bensoussan, N., Chiggiato, J., Nardelli, B.B., Pisano, A. and Garrabou, J: Insights on 2017 Marine Heat Waves in the Mediterranean Sea. Journal of Operational Oceanography (Copernicus Marine Service Ocean State Report, Issue 3), Volume: 12:sup1, 101-108, doi: 10.1080/1755876X.2019.1633075, 2019.

Caloiero, T. and Aristodemo, F.: Trend Detection of Wave Parameters along the Italian Seas. Water. 13(12):1634. doi:10.3390/w13121634, 2021.

Camus, P., Tomás, A., Izaguirre, C., Rodríguez, B., Díaz-Hernández, G. and Losada, I.: Probabilistic assessment of port operability under climate change, Coastal management, environment, and risk, doi:10.9753/icce.v36.risk.54, Nº 36, 2018.

Casas-Prat, M. and Sierra, J.P.: Trend analysis of wave direction and associated impacts on the Catalan coast. Climatic Change 115, 667–691, doi:10.1007/s10584-012-0466-9, 2012.

Cavaleri, L., Bertotti, L., Torrisi, L., Bitner-Gregersen, E., Serio, M., and Onorato, M.: Rogue waves in crossing seas: The Louis Majesty accident, J. Geophys. Res., 117, C00J10, https://doi.org/10.1029/2012JC007923, 2012.

Chiggiato et al. 2023: Recent changes in the Mediterranean Sea. In book: Oceanography of the Mediterranean Sea, An introductory guide. Elsevier 2023, 289-334. doi: 10.1016/B978-0-12-823692-5.00008-X, 2023.

https://doi.org/10.5194/sp-2023-31
Preprint. Discussion started: 29 August 2023

Clementi, E., Korres, G., Cossarini, G., Ravdas, M., Federico, I., Goglio, A.C., Salon, S., Zacharioudaki, A., Pattanaro, M. and Coppini, G.: The September 2020 Medicane Ianos predicted by the MediterraneanForecasting systems. Ocean State Report Issue 6, Journal of operational oceanography, doi:10.1080/1755876X.2022.2095169, 2022.

Costas, R., Figuero, A., Sande, J., Peña, E., and Guerra, A.: The influence of infragravity waves, wind, and basin resonance on vessel movements and related downtime at the Outer Port of Punta Langosteira, Spain. Applied Ocean Research, 129, 103370, doi:10.1016/j.apor.2022.103370, 2022.

Dayan, H., McAdam, R., Juza, M., Masina, S. and Speich, S.: Marine heat waves in the Mediterranean Sea: An assessment from the surface to the subsurface to meet national needs. Front. Mar. Sci., 10:1045138, doi: 10.3389/fmars.2023.1045138, 2023.

De Alfonso, M., García-Valdecasas, J.M., Aznar, R., Pérez-Gómez, B., Rodríguez, P., de los Santos, F.J. and Álvarez-Fanjul, E.: Record wave storm in the Gulf of Cadiz over the past 20 years and its impact on harbours. Copernicus Marine Service Ocean State Report, Issue 4, Journal of Operational Oceanography, 13:sup1, Section 4.6, S137-S144, DOI: 10.1080/1755876X.2020.1785097, 2020.

De Alfonso, M., Lin-Ye, J., García-Valdecasas, J.M., Pérez-Rubio, S., Luna, M.Y., Santos-Muñoz, D., Ruiz, M.I., Pérez-Gómez, B. and Álvarez-Fanjul. E.: Storm Gloria: sea state evolution based on in situ measurements and modelled data and its impact on extreme values. Front Mar Sci., 8:1–17, doi:10. 3389/fmars.2021.646873, 2021.

Denaxa, D., Korres, G., Sotiropoulou, M. and Lecci, R.: EU Copernicus Marine Service Product User Manual for the Mediterranean Sea Waves Reanalysis MEDSEA_MULTIYEAR_WAV_006_012, Issue: 2.2, Mercator Ocean International, https://catalogue.marine.copernicus.eu/documents/PUM/CMEMS-MED-PUM-006-012.pdf (last access: 2 June 2023), 2022.

ECCLIPSE website: https://ecclipse.eu/, last access: 18 July 2023.

EU Copernicus Marine Service Product: Atlantic Iberian Biscay Irish Ocean- In-Situ Near Real Time Observations, Mercator Ocean International [data set], https://doi.org/10.48670/moi-00043, 2022a.

EU Copernicus Marine Service Product: Mediterranean Sea Waves Reanalysis, Mercator Ocean International [data set], https://doi.org/10.25423/cmcc/medsea_multiyear_wav_006_012, 2022b.

Elgar, S., Herbers, T.H.C., Okihiro, M., Oltman-Shay, J. and Guza, R.T.: Observations of infragravity waves. J. Geophys. Res., 97 (C10), 15573–15577, 1992.

Erikson, L., Morim, J., Hemer, M. et al.: Global Ocean wave fields show consistent regional trends between 1980 and 2014 in a multi-product ensemble. Commun Earth Environ 3, 320, doi:10.1038/s43247-022-00654-9, 2022.

Eyring, V., N.P. Gillett, K.M. Achuta Rao, R. Barimalala, M. Barreiro Parrillo, N. Bellouin, C. Cassou, P.J. Durack, Y. Kosaka, S. McGregor, S. Min, O. Morgenstern, and Y. Sun, 2021: Human Influence on the Climate System. In Climate Change 2021: The Physical Science Basis. Contribution of Working Group I to the Sixth Assessment Report of the Intergovernmental Panel on Climate Change [Masson-Delmotte, V., P. Zhai, A. Pirani, S.L. Connors, C. Péan, S. Berger, N. Caud, Y. Chen, L. Goldfarb, M.I. Gomis, M. Huang, K. Leitzell, E. Lonnoy, J.B.R. Matthews, T.K. Maycock, T. Waterfield,

https://doi.org/10.5194/sp-2023-31
Preprint. Discussion started: 29 August 2023

O. Yelekçi, R. Yu, and B. Zhou (eds.)]. Cambridge University Press, Cambridge, United Kingdom and New York, NY, USA, 423–552, doi: 10.1017/9781009157896.005, 2021.

Fanti, V., Ferreira, Ó., Kümmerer, V. et al.: Improved estimates of extreme wave conditions in coastal areas from calibrated global reanalyses. Commun Earth Environ 4, 151, doi:10.1038/s43247-023-00819-0, 2023.

García-Valdecasas, J., Pérez Gómez, B., Molina, R. et al.: Operational tool for characterizing high-frequency sea level oscillations, Nat Hazards, 106, 1149–1167, doi:10.1007/s11069-020-04316-x, 2021.

Garrabou, J., Gómez-Gras, D., Medrano, A. et al.: Marine heatwaves drive recurrent mass mortalities in the Mediterranean Sea. Global Change Biology, 28, 5708– 5725, doi:10.1111/gcb.16301, 2022.

Giesen, R., Clementi, E., Bajo, M., Federico, I., Stoffelen, A. and Santoleri, R.: The November 2019 record high water levels in Venice, Italy. Journal of Operational Oceanography (Copernicus Marine Service Ocean State Report, Issue 5), Volume: 14:sup1, 156-162, doi: 10.1080/1755876X.2021.1946240, 2021.

Goda, Y.: On the methodology of selecting design wave height. Coastal Engineering Proceedings, 1(21), 1988.

Gómez Lahoz, G. and Carretero Albiach, J.C.: Wave forecasting at the Spanish coasts, Journal of Atmospheric and Ocean Science, 10:4, 389-405, doi: 10.1080/17417530601127522, 2005.

Guizien, K.: Spatial variability of wave conditions in the Gulf of Lions (NW Mediterranean Sea). Vie et milieu - life and environment, 59 (3/4): 261-270, 2009.

Gutiérrez-Serret, R., Grassa, J.M., Grau, J.I.: Breakwater development in Spain. The last ten years. Proceeding presented at Coasts, Marine Structures and Breakwaters: Adapting to Change, 9th International Conference organised by the Institution of Civil Engineers, Edinburgh, Scotland, UK, 16-18 September 2009.

Haigh, R., Amaratunga, D. and Hemachandra, K.: A capacity analysis framework for multi-hazard early warning in coastal communities. Procedia Engineering, 212, 1139-1146, doi:10.1016/j.proeng.2018.01.147, 2018.

Hochman, A., Marra, F., Messori, G., Pinto, J.G., Raveh-Rubin, S., Yosef, Y. and Zittis, G. Extreme weather and societal impacts in the eastern Mediterranean. Earth System Dynamics, 13, 749-777, doi:10.5194/esd-13-749-2022, 2022.

Inch, K., Davidson, M., Masselink, G. and Russell,P.: Observations of nearshore infragravity wave dynamics under high energy swell and wind-wave conditions, Continental Shelf Research, 138, 19-31, doi:10.1016/j.csr.2017.02.010, 2017.

In Situ TAC partners: EU Copernicus Marine Service Product User Manual for the Atlantic Iberian Biscay Irish Ocean- In-Situ Near Real Time Observations, INSITU_IBI_PHYBGCWAV_DISCRETE_MYNRT_013_033, Issue: 1.14, Mercator Ocean International, https://catalogue.marine.copernicus.eu/documents/PUM/CMEMS-INS-PUM-013-030-036.pdf (last access: 2 June 2023), http://dx.doi.org/10.13155/43494, 2022.

Intergovernmental Panel on Climate Change (IPCC). The Ocean and Cryosphere in a Changing Climate: Special Report of the Intergovernmental Panel on Climate Change. Cambridge: Cambridge University Press. doi:10.1017/9781009157964, 2022.

Izaguirre, C., Losada, I.J., Camus, P. et al.: Climate change risk to global port operations. Nat. Clim. Chang., 11, 14–20, doi:10.1038/s41558-020-00937-z, 2021.

https://doi.org/10.5194/sp-2023-31
Preprint. Discussion started: 29 August 2023

Juza, M. and Tintoré, J.: Multivariate Sub-Regional Ocean Indicators in the Mediterranean Sea: From Event Detection to Climate Change Estimations, Front. Mar. Sci., 8, 610589, https://doi.org/10.3389/fmars.2021.610589, 2021.

Kendall, M.G. Rank Correlation Methods; Hafner Publishing Company: New York, NY, USA, 1962.

Kokkini, Z. and Notarstefano, G.: Unusual salinity pattern in the South Adriatic Sea in 2016. Copernicus Marine Service Ocean State Report, Journal of Operational Oceanography, 11:sup1, S130-S131, doi: 10.1080/1755876X.2018.1489208, 2018.

Konisky, D. M., Hughes, L., and Kaylor, C.H.: Extreme weather events and climate change concern. Clim. Change, 134, 533–547, doi: 10.1007/s10584-015-1555-3, 2015.

Linnenluecke, M. K., Griffiths, A., and Winn, M.: Extreme weather events and the critical importance of anticipatory adaptation and organizational resilience in responding to impacts. Bus. Strat. Environ., 21, 17–32, doi: 10.1002/bse.708, 2012.

López, M. and Iglesias, G.: Long wave effects on a vessel at berth, Applied Ocean Research, 47, 63-72, doi:10.1016/j.apor.2014.03.008, 2014.

Lorente, P., Lin-Ye, J., García-León, M., Reyes, E., Fernandes, M., Sotillo, M.G., Espino, M., Ruiz, M. I., Gracia, V., Pérez, S., Aznar, R., Alonso-Martirena, A., and Álvarez-Fanjul, E.: On the Performance of High Frequency Radar in the Western Mediterranean During the Record-Breaking Storm Gloria, Front. Mar. Sci., 8, 645762, doi:10.3389/fmars.2021.645762, 2021.

McComb, J.: Modelling long wave generation and propagation around and within ports. Proc. 2011 Coasts and Ports Conf. Perth, Australia, 2011.

McComb, P., Zyngfogel, R., and Pérez-Gomez, B.: Predicting infragravity waves in harbours - an evaluation of published equations and their use in forecasting operational thresholds, Coastal Engineering Proceedings, 36v, waves.7, doi:10.9753/icce.v36v.waves.7, 2020.

Mann, H.B. Nonparametric tests against trend. Econometrica, 13, 245–259, 1945.

Milglietta, M. M. and Rotunno, R.: Development mechanisms for Mediterranean tropical-like cyclones (medicanes), Q. J. Roy. Meteorol. Soc., 145, 1444–1460, 2019.

Morales-Márquez, V., Orfila, A., Simarro, G., and Marcos, M.: Extreme waves and climatic patterns of variability in the Eastern North Atlantic and Mediterranean Basins. Ocean Sci., 16, 1385–1398, doi: 10.5194/os-16-1385-2020, 2020.

Naseef, T.M., Kumar, V.S., Joseph, J. et al.: Uncertainties of the 50-year wave height estimation using generalized extreme value and generalized Pareto distributions in the Indian Shelf seas, Nat Hazards 97, 1231–1251, doi:10.1007/s11069-019-03701-5, 2019.

Notarstefano, G., Menna, M. and Legeais, J.F.: Reversal of the Northern Ionian circulation in 2017. Ocean State Report 3, Journal of Operational Oceanography, 12:sup1, S108-S111, doi: 10.1080/1755876X.2019.1633075, 2019.

Okihiro, M., Guza, R.T. and Seymour, R.J.: Excitation of seiche observed in a small harbor. J. Geophys. Res., 98, 18.201–18.211, 1993.

https://doi.org/10.5194/sp-2023-31
Preprint. Discussion started: 29 August 2023

Pérez-Gómez, B., Vela, J., and Alvarez-Fanjul, E.: A new concept of multi- purpose sea level station: example of implementation in the REDMAR network. In: Proceedings of the Fifth International Conference on EuroGOOS, May 2008: Coastal to global operational oceanography: achievements and challenges, Exeter, 2008.

Pérez-Gómez, B., García-León, M., García-Valdecasas, J., Clementi, E., Mösso Aranda, C., Pérez-Rubio, S., Masina, S., Coppini, G., Molina-Sánchez, R., Muñoz-Cubillo, A., García Fletcher, A., Sánchez González, J.F., Sánchez-Arcilla, A. and Álvarez-Fanjul, E.: Understanding Sea Level Processes During Western Mediterranean Storm Gloria. Front. Mar. Sci. 8:647437. doi: 10.3389/fmars.2021.647437, 2021.

Portillo Juan, N., Negro Valdecantos, V., del Campo, J.M.: Review of the Impacts of Climate Change on Ports and Harbours and Their Adaptation in Spain. Sustainability, 14, 7507, doi:10.3390/su14127507, 2022.

Radovic, V., and Iglesias, I.: Extreme weather events: definition, classification and guidelines towards vulnerability reduction and adaptation management. Good Health Well Being, 68, 1–13, doi: 10.1007/978-3-319- 71063-1_68-1, 2018.

Ramirez-Llodra, E., De Mol, B., Company, J.B., Coll, M. and Sardà, F.: Effects of natural and anthropogenic processes in the distribution of marine litter in the deep Mediterranean Sea, Progress in Oceanography, 118, 273-287, doi:10.1016/j.pocean.2013.07.027, 2013.

Ribeiro, A.S., Lopes, C.L., Sousa, M.C., Gómez-Gesteira, M., Vaz, N., Dias, J.M. Reporting Climate Change Impacts on Coastal Ports (NW Iberian Peninsula): A Review of Flooding Extent. J. Mar. Sci. Eng., 11, 477, doi:10.3390/jmse11030477, 2023.

Romano-Moreno, E., Diaz-Hernandez, G., Lara, J.L. Tomás, A. and Jaime, F.F.: Wave downscaling strategies for practical wave agitation studies in harbours, Coastal Engineering, 175, 104140, ISSN 0378-3839, doi:10.1016/j.coastaleng.2022.104140, 2022.

Salvadori, G., Durante, F. and De Michele, C.: Multivariate return period calculation via survival functions. Water Resour. Res., 49, 2308–2311, doi:10.1002/wrcr.20204, 2013.

Samper, Y., Liste, M., Mestres, M., Espino, M., Sánchez-Arcilla, A., Sospedra, J., González-Marco, D., Ruiz, M.I., Álvarez Fanjul, E.: Water Exchanges in Mediterranean Microtidal Harbours, Water, 14 (13), doi:10.3390/w14132012, 2022.

Sánchez-Arcilla, A., Sierra, J.P., Brown, S., Casas-Prat, M., Nicholls, R.J., Lionello, P., and Conte, D.: A review of potential physical impacts on harbours in the Mediterranean Sea under climate change, Reg Environ Change, 16, 2471–2484, doi:10.1007/s10113-016-0972-9, 2016a.

Sánchez-Arcilla, A., García-León, M., Gracia, V., Devoy, R., Stanica, A., and Gault, J.: Managing coastal environments under climate change: Pathways to adaptation. Sci. Total Environ., 572, 1336–1352, doi: 10.1016/j.scitotenv.2016.01.124, 2016b.

Scicchitano, G., Scardino, G., Monaco, C., Piscitelli, A., Milella, M., De Giosa, F. and Mastronuzzi, G.: Comparing impact effects of common storms and Medicanes along the coast of south-eastern Sicily, Marine Geology, 439, 106556, ISSN 0025-3227, doi:10.1016/j.margeo.2021.106556, 2021.

Sen, P.K. Estimates of the regression coefficient based on Kendall's tau. J. Am. Stat. Assoc., 63, 1379–1389, 1968.

https://doi.org/10.5194/sp-2023-31
Preprint. Discussion started: 29 August 2023

Sierra, J. P., Casas-Prat, M., Virgili, M., Mösso, C., and Sánchez-Arcilla, A.: Impacts on wave-driven harbour agitation due to climate change in Catalan ports, Nat. Hazards Earth Syst. Sci., 15, 1695–1709, doi:10.5194/nhess-15-1695-2015, 2015.

Sierra, J.P., Genius, A. Lionello, P. Mestres, M. Mösso, C. and Marzo, L.: Modelling the impact of climate change on harbour operability: The Barcelona port case study, Ocean Engineering, 141, 64-78, doi:10.1016/j.oceaneng.2017.06.002, 2017.

Sotillo, M.G., Mourre, B., Mestres, M., Lorente, P., Liste, M., Aznar, R., et al.: How did existing operational ocean circulation models forecast a (record-breaking) Western Mediterranean Extreme Event? Front. Mar. Sci. 81–23. doi: 10.1016/j.apor.2011.09.001, 2021.

Soussi, A., Bersani, C., Sacile, R., Bouchta, D., El Amarti, A., Seghiouer, H., Nachite, D., and Al Miys, J.: Coastal Risk Modelling for Oil Spill in The Mediterranean Sea, Advances in Science, Technol. Eng. Syst. J., 5, 273–286, 2020.

Stockdon, H.F., Holman, R.A., Howd, P.A. and Sallenger Jr, A.H.: Empirical parameterization of setup, swash and runup. Coast. Eng., 53, 573–588, 2006.

Todd, D., Blanksby, A. and Schepis, J.: Verification of design life exposure and performance of a berm breakwater, Coastal Engineering, 2012.

Tuel, A. and Eltahir, E.A.B.: Why Is the Mediterranean a Climate Change Hot Spot?, J. Climate, 33, 5829–5843, doi:10.1175/JCLI-D-19-0910.1, 2020.

Vanem, E., Fazeres-Ferradosa, T., Rosa-Santos, P. and Taveira-Pinto, F.: Statistical description and modelling of extreme ocean wave conditions. Proceedings of the Institution of Civil Engineers - Maritime Engineering, 172:4, 124-132, 2019.

Vannucchi, V., Taddei, S., Capecchi, V., Bendoni, M., Brandini, C.: Dynamical Downscaling of ERA5 Data on the North-Western Mediterranean Sea: From Atmosphere to High-Resolution Coastal Wave Climate. Journal of Marine Science and Engineering, 9(2):208, doi:10.3390/jmse9020208, 2021.

Verschuur, J., Koks, E.E. & Hall, J.W. Ports' criticality in international trade and global supply-chains. Nat Commun., 13, 4351, doi:10.1038/s41467-022-32070-0, 2022.

Verschuur, J., Koks, E.E., Li, S. et al.: Multi-hazard risk to global port infrastructure and resulting trade and logistics losses. Commun Earth Environ, 4, 5, doi:10.1038/s43247-022-00656-7, 2023.

WCPR website https://www.wcrp-climate.org/gc-extreme-events, last access: 18 July 2023.

Wehde, H., Schuckmann, K.V., Pouliquen, S., Grouazel, A., Bartolome, T., Tintore, J., De Alfonso Alonso-Muñoyerro, M., Carval, T., Racapé, V. and the INSTAC team: EU Copernicus Marine Service Quality Information Document for the Atlantic Iberian Biscay Irish Ocean- In-Situ Near Real Time Observations, INSITU_IBI_PHYBGCWAV_DISCRETE_MYNRT_013_033, Issue 2.2, Mercator Ocean International, https://catalogue.marine.copernicus.eu/documents/QUID/CMEMS-INS-QUID-013-030-036.pdf (last access: 2 June 2023), 2022.

https://doi.org/10.5194/sp-2023-31
Preprint. Discussion started: 29 August 2023

Wolff, C., Vafeidis, A. T., Muis, S., Lincke, D., Satta, A., Lionello, P., Jimenez, J. A., Conte, D., and Hinkel, J. A.: Mediterranean coastal database for assessing the impacts of sea-level rise and associated hazards, Sci. Data, 5, 180044, doi:10.1038/sdata.2018.44, 2018.

Zacharioudaki, A., Ravdas, M., Korres, G., and Goglio, A.C.: EU Copernicus Marine Service Quality Information Document for the Mediterranean Sea Waves Reanalysis. MEDSEA_MULTIYEAR_WAV_006_012, Issue: 2.2, Mercator Ocean International, https://catalogue.marine.copernicus.eu/documents/QUID/CMEMS-MED-QUID-006-012.pdf (last access: 2 June 2023), 2022a.

Zacharioudaki, A., Ravdas, M. and Korres, G.: Wave climate extremes in the Mediterranean Sea obtained from a wave reanalysis for the period 1993-2000. Ocean state Report, Issue 6, Journal of Operational Oceanography, 2022b.

Tables

Product ref. no.	**Product ID & type**	**Data access**	**Documentation**
1	ERA5 global reanalysis, numerical models	Copernicus Climate Data Store: https://cds.climate.copernicus.eu/cdsapp#!/dataset/reanalysis-era5-single-levels?tab=form	Product description: https://confluence.ecmwf.int/display/CKB/ERA5%3A+data+documentation
2	Puertos del Estado regional wave forecast model, numerical models	Puertos del Estado: https://portus.puertos.es https://portuscopia.puertos.es/	Product description: Gómez Lahoz and Carretero Albiach, 2005. https://www.puertos.es/es-es/Documents/Descripcion_Pred_Oleaje_en.pdf

https://doi.org/10.5194/sp-2023-31
Preprint. Discussion started: 29 August 2023

3	2Hz data, high frequency sea level oscillations and agitation parameters from Melilla tide-gauge, in situ observations	Puertos del Estado websites: https://portus.puertos.es https://portuscopia.puertos.es/Catalog http://opendap.puertos.es/thredds/catalog/tidegauge_meli/catalog.html	Product description: García Valdecasas et al. (2021) https://bancodatos.puertos.es/BD/informes/INT_3.pdf
4	INSITU_IBI_PHYBGCWAV_DISCRETE_MYNRT_013_033, in situ observations	EU Copernicus Marine Service Product (2022a)	PUM: In situ TAC partners (2022); QUID: Wehde et al. (2022)
5	MEDSEA_MULTIYEAR_WAV_006_012, numerical models	EU Copernicus Marine Service Product (2022b)	PUM: Denaxa et al. (2022); QUID: Zacharioudaki et al. (2022a)

Table 1. Products from the Copernicus Marine Service and other complementary datasets used in this study, including the Product User Manual (PUM) and QUality Information Document (QUID). For complementary datasets, the link to the product description, data access and scientific references are provided. Last access for all web pages cited in this table: 12 June 2023.

Work	Extreme event	Year	Location	Issue
Kokkini et al. (2018)	Anomaly of salinity	2016	Adriatic Sea	2
Bensoussan et al. (2019)	Marine heat wave	2017	Mediterranean Sea	3
Notarstefano et al. (2019)	Current reversal	2017	Ionian Sea	3
De Alfonso et al. (2020)	Emma Storm	2018	Gulf of Cadiz	4
Berta et al. (2020)	Extreme wind	2018	Ligurian Sea	4
Giesen et al. (2021)	Sea level rise	2019	Adriatic Sea	5
Álvarez-Fanjul et al. (2022)	Storm Gloria	2020	NW Mediterranean Sea	6

https://doi.org/10.5194/sp-2023-31
Preprint. Discussion started: 29 August 2023

Clementi et al. (2022)	Medicane Ianos	2020	Ionian Sea	6

Table 2. Summary of recent studies (published in previous issues of the Ocean State Report) dealing with extreme metocean events in the Mediterranean Sea and adjacent areas.

Physical processes	Specific impacts	General impacts
Nonlinear interactions of wind short waves (5-30 s)	Excessive vessel motions at berth	Unsafe operations
Infragravity (IG) long waves (30-600 s)	Restriction of (un)load operations	Inefficient port management
Resonance (seiche)	Break of mooring lines / fenders	Downtime of the facility
Large water level fluctuations and strong horizontal currents	Ship collision	Interruption of supply chain
	Damage to vessels / port facilities	Economic losses

Table 3. Conceptual landscape of potential impacts on harbour operations and infrastructures during severe wave storms.

Parameter	Location	Coverage	Mean	Std	P50	P90	P99	P99.9
SWH (m)	coastal	2008-2022	0.69	0.59	0.49	1.44	2.92	4.44
mean period (s)	coastal	2008-2022	3.80	0.87	3.73	4.93	6.29	7.27
IG_{max} (m)	port	2015-2022	0.08	0.05	0.06	0.14	0.28	0.44
agitation (m)	port	2015-2022	0.1	0.07	0.08	0.17	0.38	0.6

Table 4. Basic statistics (mean, standard deviation, and diverse percentiles) for the significant wave height (SWH) and mean wave period hourly observations provided by Melilla coastal buoy (magenta square in Figure 1, b-c) for the period between 1 April 2008 and 31 December 2022. Infragravity waves maximum heigth (IG_{max}) and agitation data were provided by Melilla tide-gauge (magenta dot in Figure 1, b-c) for the entire period 2015-2022.

https://doi.org/10.5194/sp-2023-31
Preprint. Discussion started: 29 August 2023

Parameter (unit)	2010-2020	2010-2022
Exceedance threshold (m)	2	2
Minimum time between storms (days)	5	5
Mean number of storms per year	9.73	10.12
Weibull distribution: alpha	1.82	1.90
Weibull distribution: beta	1.13	1.10
Weibull distribution: gamma	1.14	1.07
Return period for events with SWH = 3 m (years)	1.03	1.02
Return period for events with SWH = 4 m (years)	1.45	1.34
Return period for events with SWH = 5 m (years)	3.19	2.59
Return period for events with SWH = 6 m (years)	9.24	6.4
Return period for events with SWH = 7 m (years)	30.41	17.75
Return period for events with SWH = 8 m (years)	106.4	51.79

Table 5. Return period computed for two different periods, as derived from hourly in situ observations from Melilla coastal buoy. The long-term extreme sea state was characterised by using the Peak Over Threshold method with the fitting of a Three-Parameter Weibull probability distribution to the SWH observations.

IG wave height	Warning	Reactivity
< 0.10 m	Safe	Business as usual, well-tendered vessels
– 0.15 m	Caution	Additional management recommended
> 0.15 m	Extreme caution	Active management required
> 0.20 m	Danger	Evacuation of vessels from berths, port downtime

635 **Table 6. Infragravity (IG) wave height thresholds used for port management.**

https://doi.org/10.5194/sp-2023-31
Preprint. Discussion started: 29 August 2023

Figures

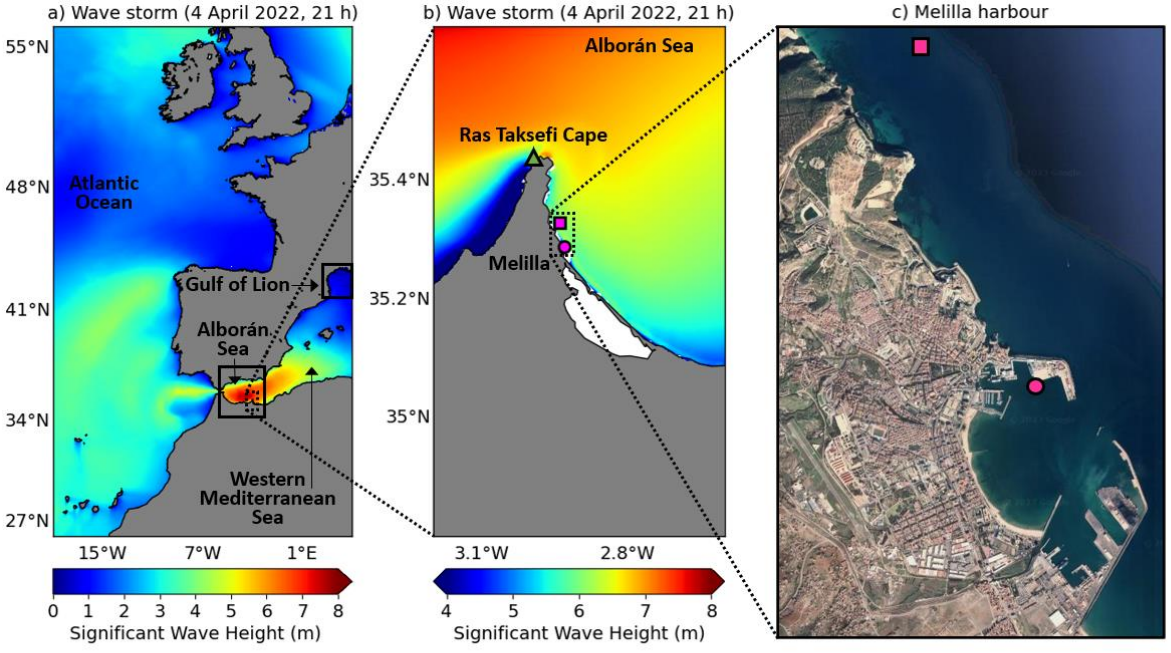

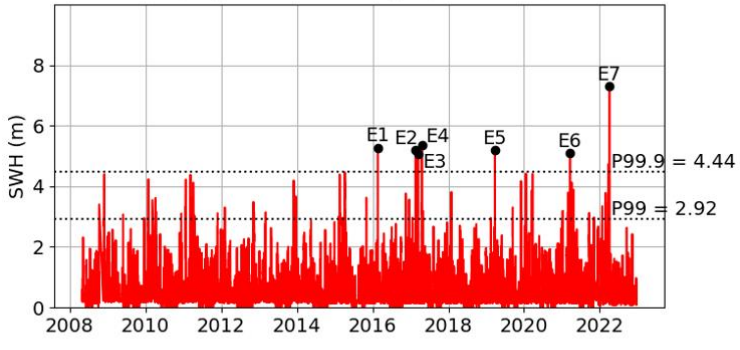

Event	Date (hour)	SWH (m)	Period (s)	Dir (°)
E1	2016-02-21 (00)	5.25	7.15	63
E2	2017-02-21 (02)	5.21	6.83	66
E3	2017-03-15 (01)	5.05	6.99	51
E4	2017-04-21 (15)	5.36	7.03	69
E5	2019-03-27 (00)	5.21	6.88	69
E6	2021-03-20 (21)	5.09	6.91	55
E7	2022-04-04 (21)	7.32	9.30	55

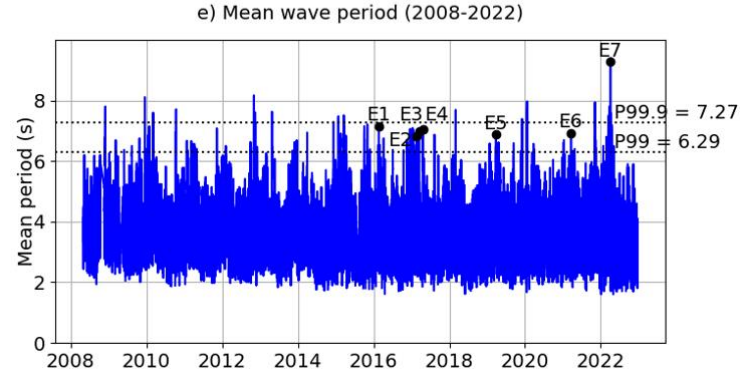

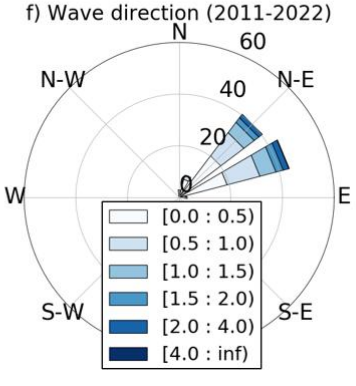

https://doi.org/10.5194/sp-2023-31
Preprint. Discussion started: 29 August 2023

Figure 1. Wave storm in the SW Mediterranean Sea. Hourly map (4 of April 2022, 21 h local time) of significant wave height (SWH) at synoptic (a) and coastal (b) scales during the peak storm as predicted by the wave forecast model of Puertos del Estado -product ref. no. 2 (Table 1)-. Green triangle indicates the location of Ras Taksefi Cape; c) © Google map illustrating the geometry and details of Melilla harbour. Magenta dot and square represent the tide-gauge and coastal buoy location, respectively; d) hourly timeseries of SWH recorded at Melilla coastal buoy for 2008-2022 -product ref. no. 4 (Table 1)-. Black dots indicate those SWH events above 99.9th (P99.9) and 99th (P99) percentiles, represented by horizontal black dotted lines. Table on the right gathers details about each event; e) Hourly timeseries of mean wave period for 2008-2022 -product ref. no. 4 (Table 1)-; f) Wave rose illustrating the main incoming directions during the time period 2011-2022 -product ref. no. 4 (Table 1).

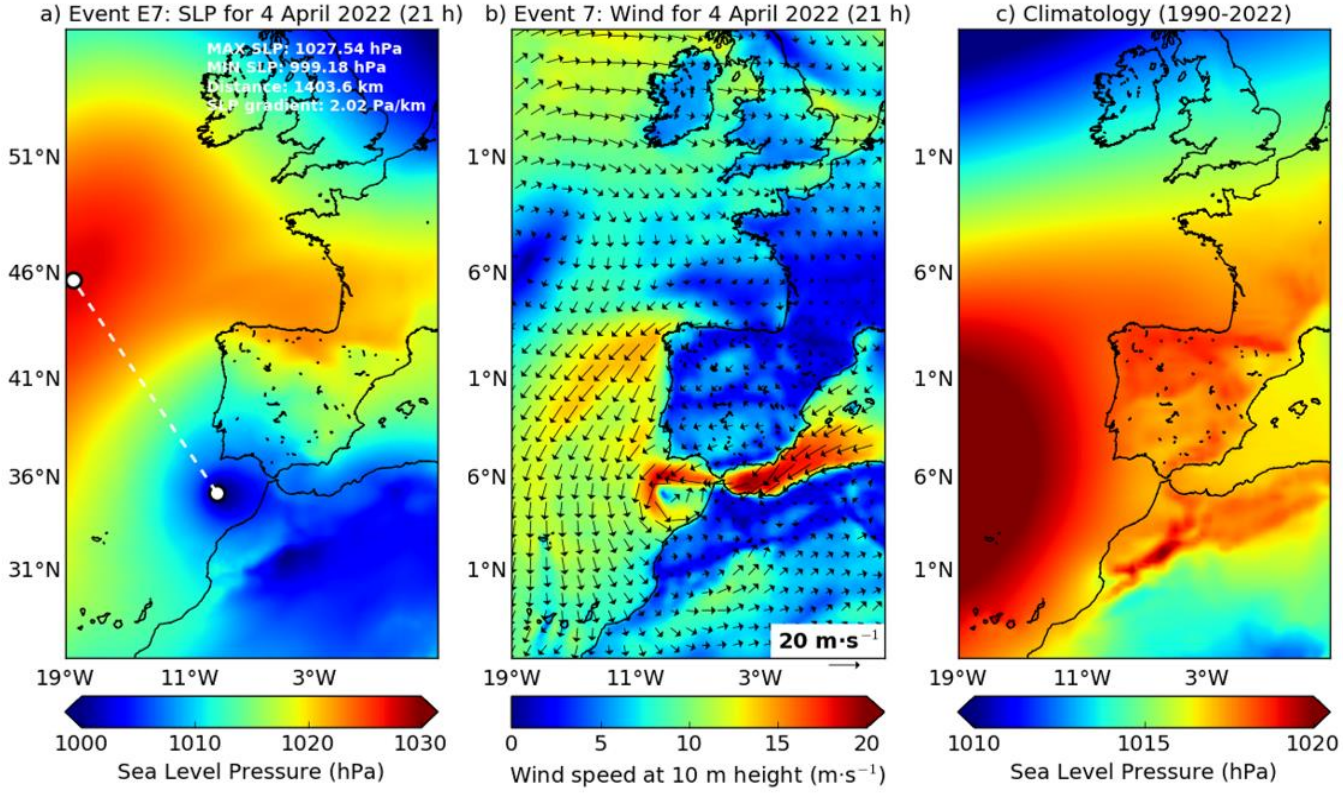

Figure 2. (a-b) Hourly synoptic patterns of sea level pressure (SLP) and wind at 10 m during the extreme event E7; c) Climatology (1990-2022) of SLP. Maps derived from ERA5 reanalysis -product ref. no. 1 (Table 1).

https://doi.org/10.5194/sp-2023-31
Preprint. Discussion started: 29 August 2023

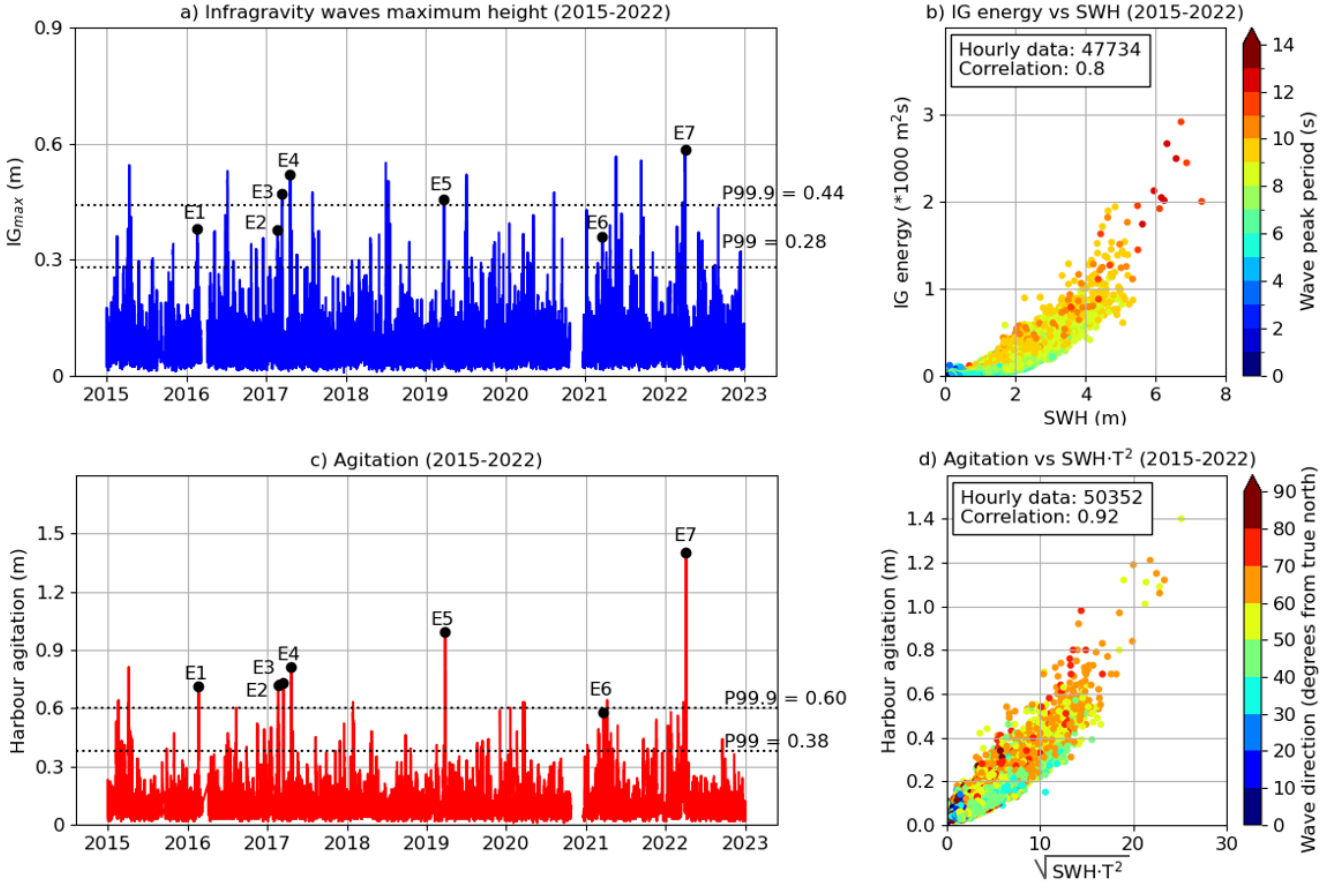

Figure 3. a) Hourly timeseries of infragravity (IG) wave maximum height for the period 2015-2022 (product ref. no. 3 in Table 1), as registered by Melilla tide gauge (Figure 1, a-b). The seven extreme events analysed in this work are denoted by black dots; b) Scatter plot of the energy in the IG band against hourly wave observations from Melilla coastal buoy (SWH and peak period); c) Hourly timeseries of agitation inside the harbour for the period 2015-2022 (product ref. no. 3 in Table 1); d) Scatter plot of the harbour agitation against the wave conditions outside the harbour (SWH and wave direction).

https://doi.org/10.5194/sp-2023-31
Preprint. Discussion started: 29 August 2023

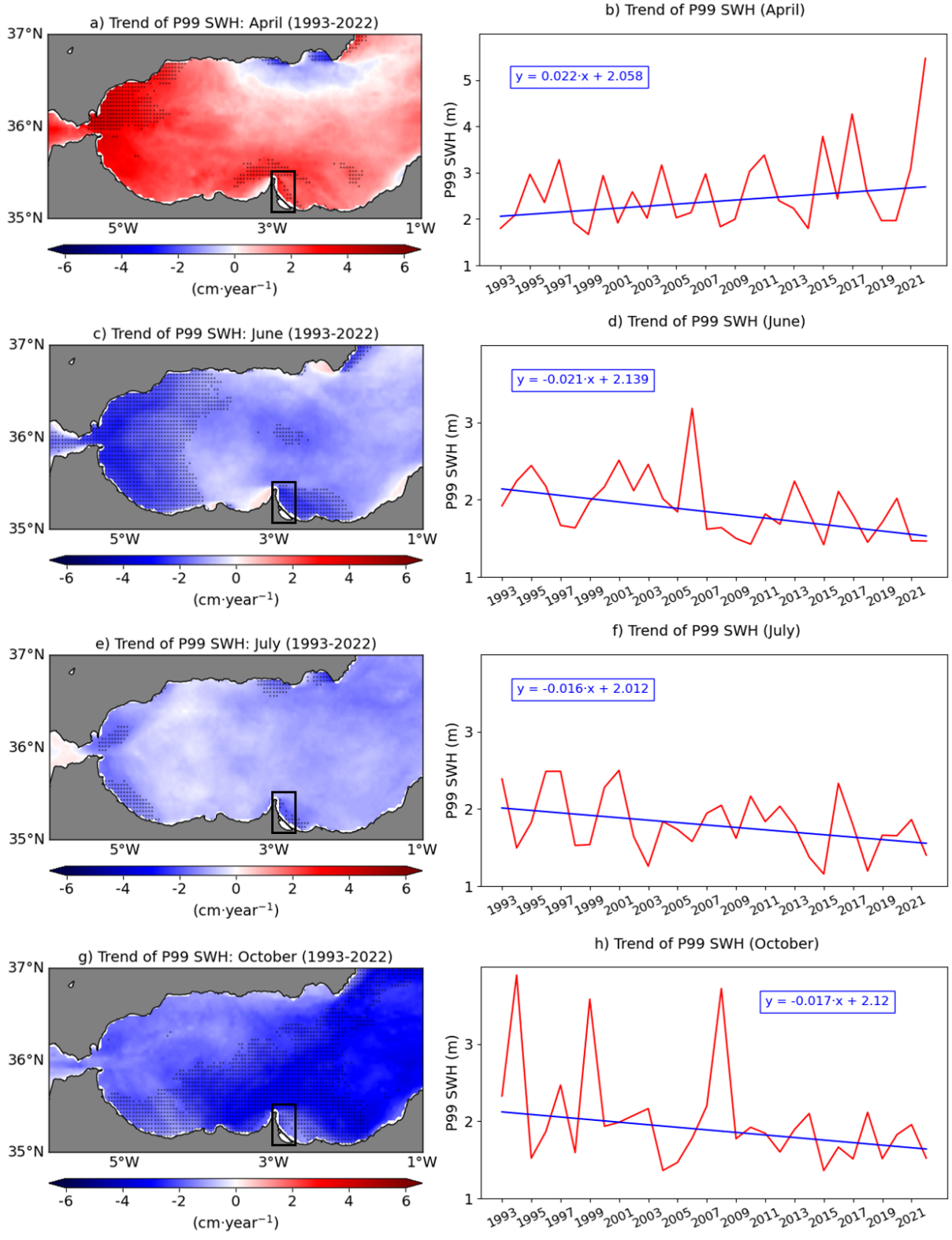

https://doi.org/10.5194/sp-2023-31
Preprint. Discussion started: 29 August 2023

Figure 4. Left column: monthly trend maps of the 99th percentile (P99) of significant wave height (SWH) over the Alborán Sea for the 1993-2022 period as derived from a regional wave reanalysis -product ref. no. 5 (Table 1)-. Areas with statistically significant trends at the 90% confidence intervals are denoted by black dots. Right column: temporal trends, computed over the Melilla subdomain (represented by a black box in the associated maps).

https://doi.org/10.5194/sp-2023-31
Preprint. Discussion started: 29 August 2023

Annex

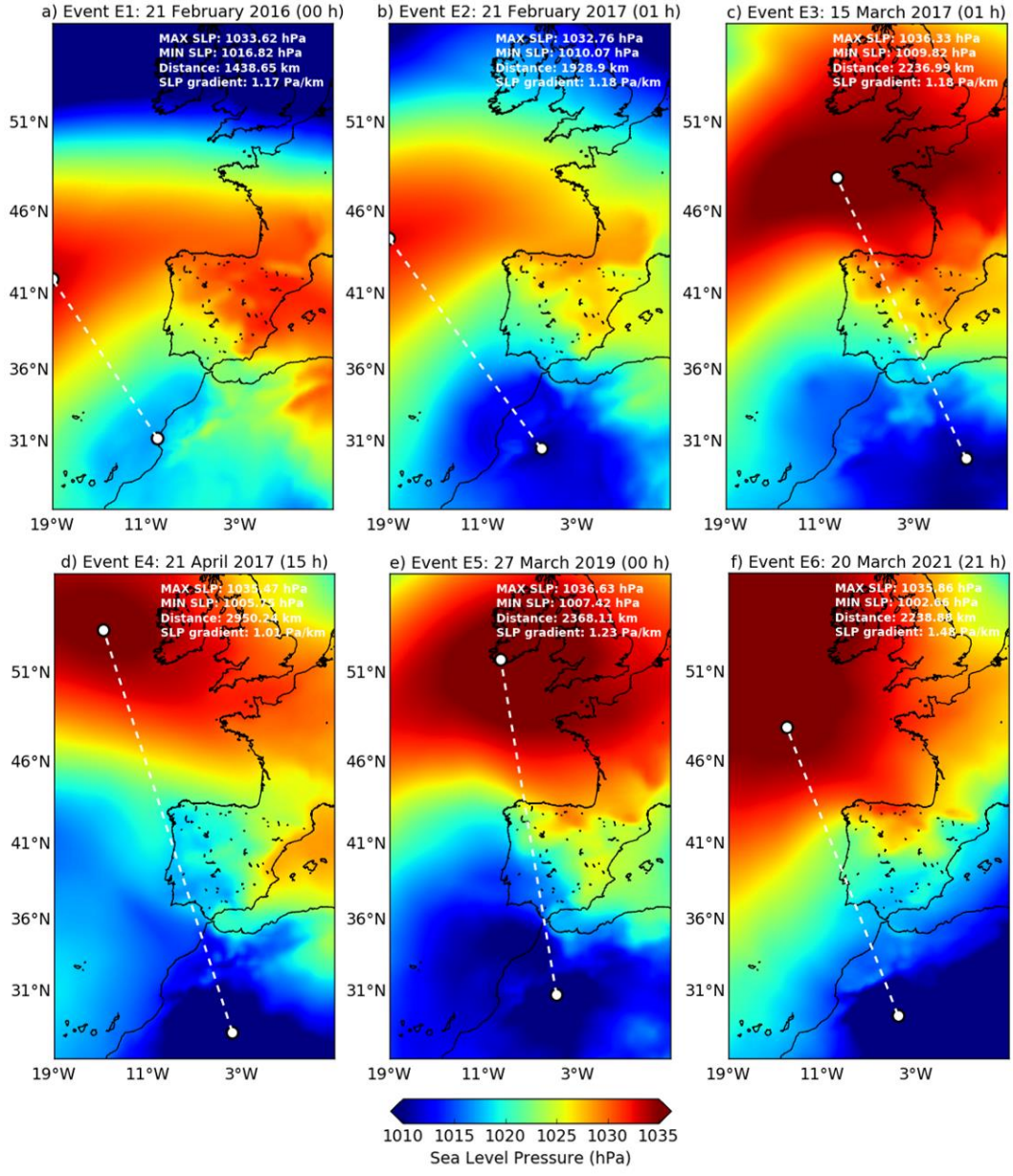

Annex 1. Hourly synoptic patterns of sea level pressure (SLP) corresponding to the 6 extreme wave events detected before the study case and listed in Figure 1d. Maps derived from ERA5 reanalysis -product ref. no. 1 (Table 1)-. Maximum and minimum values of SPL are marked with white dots and the SLP gradient is indicated in the lower right corner. The hour represents local time.

https://doi.org/10.5194/sp-2023-31
Preprint. Discussion started: 29 August 2023

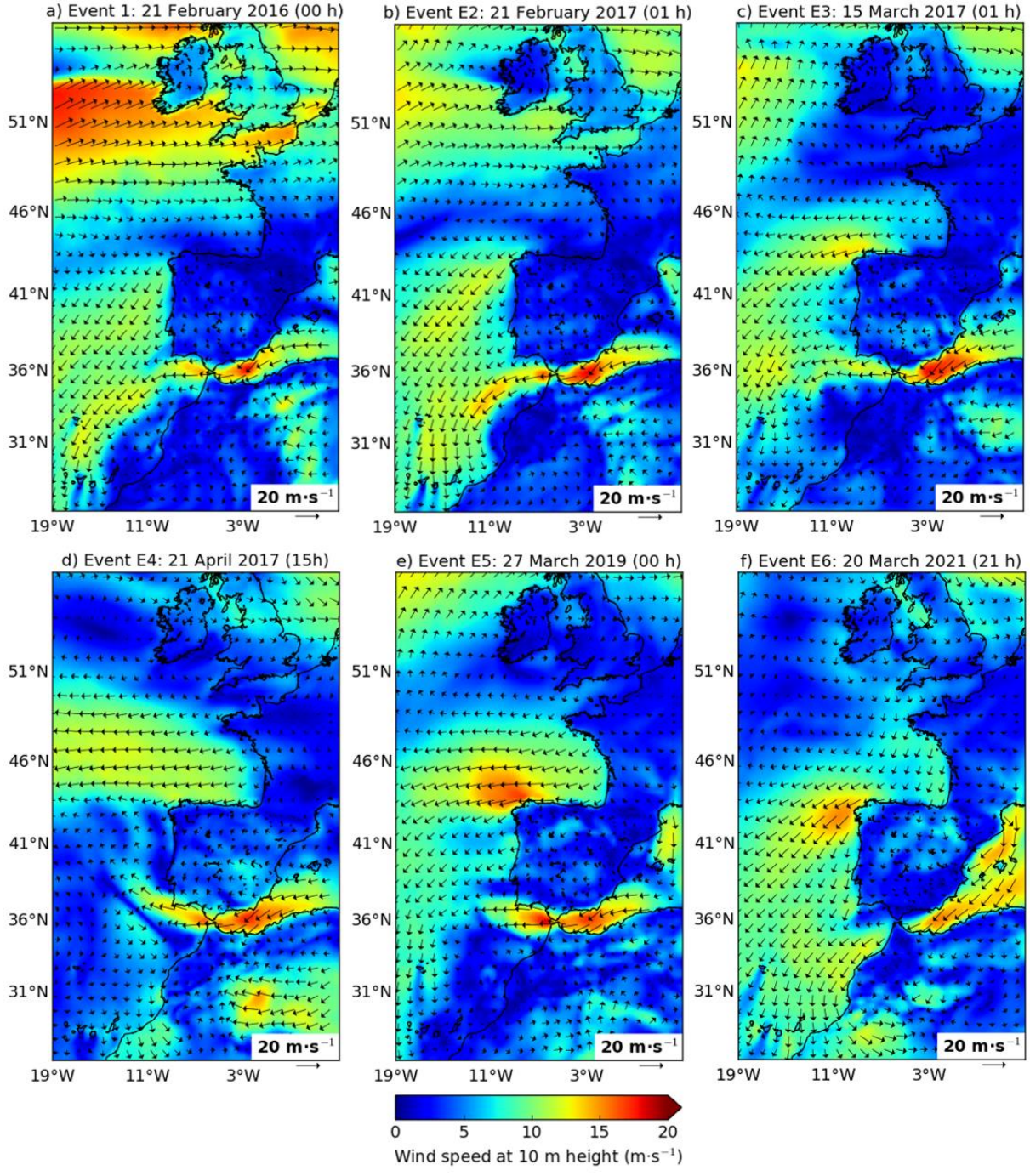

680

Annex 2. Hourly synoptic patterns of wind at 10 m height corresponding to the 6 extreme wave events detected before the study case and listed in Figure 1d. Maps derived from ERA5 reanalysis -product ref. no. 1 (Table 1)-.

https://doi.org/10.5194/sp-2023-31
Preprint. Discussion started: 29 August 2023

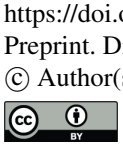

a) Scatterplot of SWH in Melilla (Jan 2009 - Dec 2022)

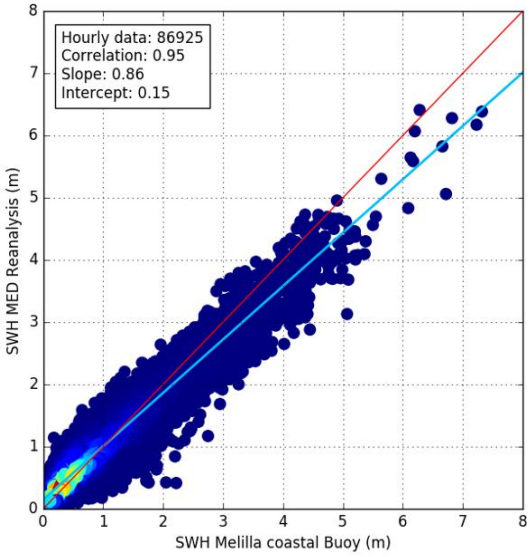

b) P99 of significant wave height (1993-2022)

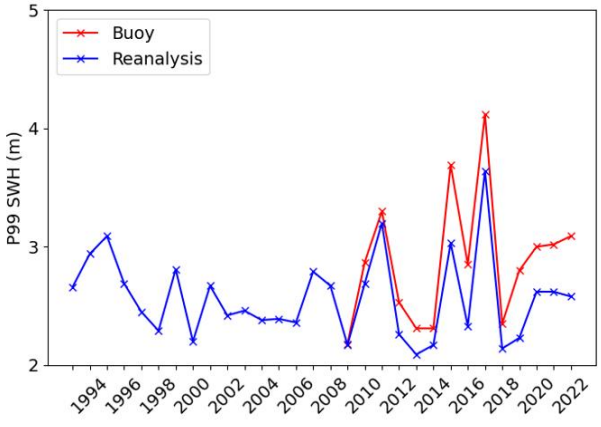

c) Monthly P99 of significant wave height

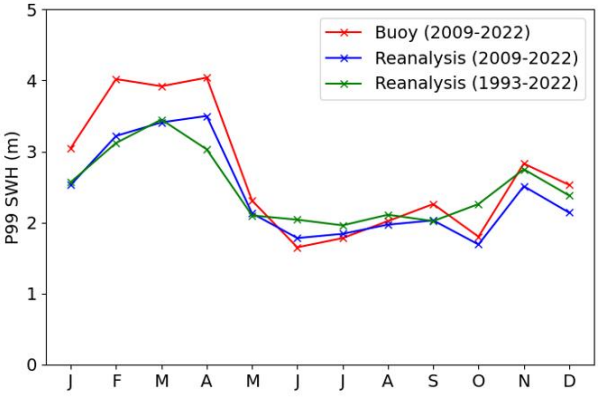

https://doi.org/10.5194/sp-2023-31
Preprint. Discussion started: 29 August 2023

Annex 3. a) Skill assessment of the regional wave reanalysis -product ref. no. 5 (Table 1)- against Melilla coastal buoy -product ref. no. 4 (Table 1)-: best linear fit of scatter plot between hourly in situ observations of significant wave height (SWH) and modelled outputs in the grid point closest to the moored buoy for a 14-year period (2009-2022). Statistical metrics are adhered in white box; b) Annual values of observed (red line) and modelled (blue line) P99 of SWH in Melilla; c) Monthly values of observed (red line: 2009-2022) and modelled (blue line for 2009-2022, green line for 1993-2022) P99 of SWH in Melilla.

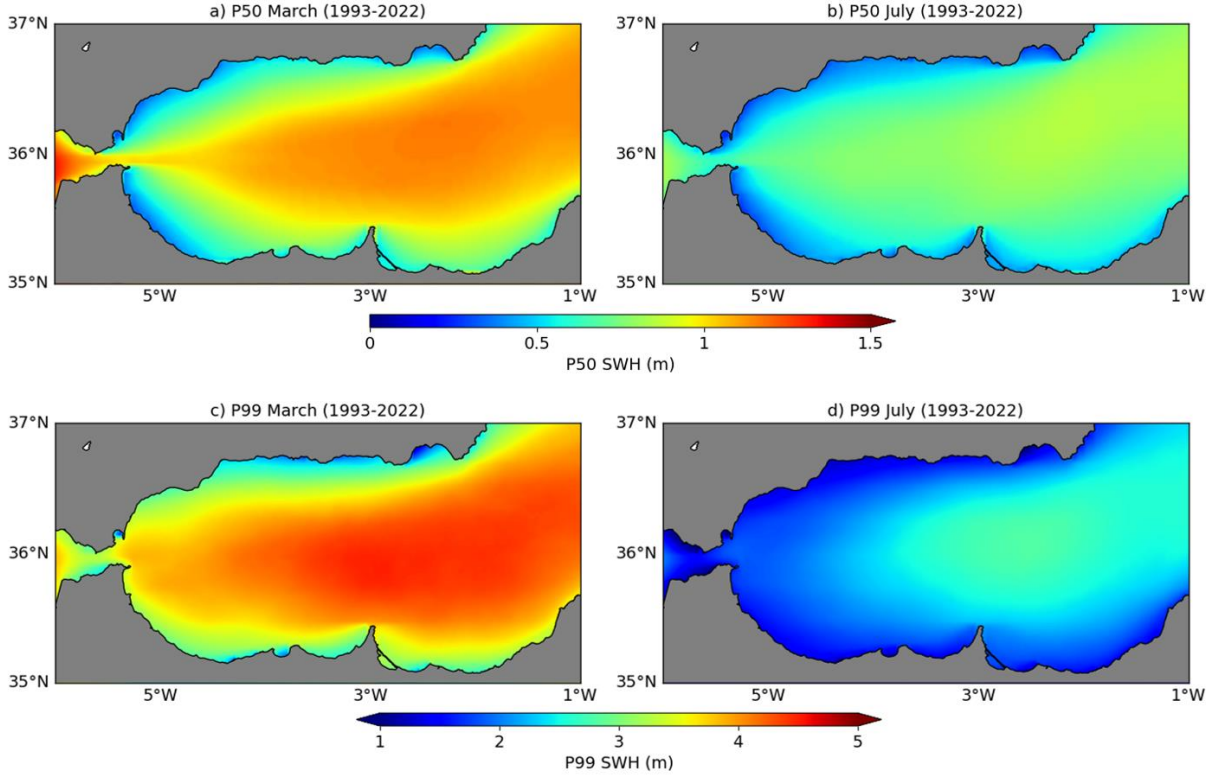

Annex 4. Spatial distribution of the 50th -P50- (a-b) and 99th -P99- (c-d) percentiles of significant wave height (SWH) over the Alborán Sea for January (left column) and July (right column), as derived from the regional wave reanalysis product for the 1993-2022 period -product ref. no. 5 (Table 1)-.

https://doi.org/10.5194/sp-2023-31
Preprint. Discussion started: 29 August 2023

700

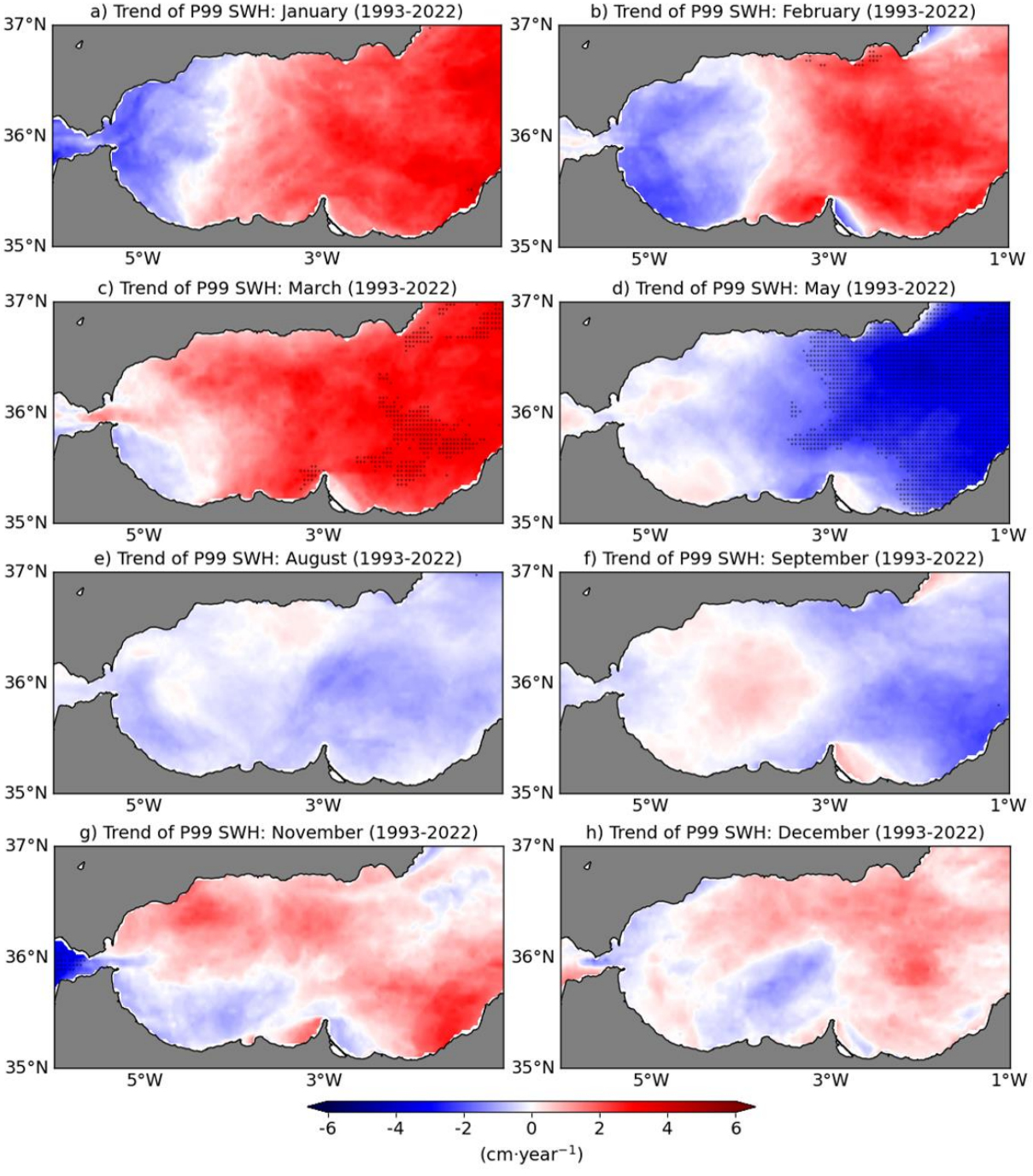

https://doi.org/10.5194/sp-2023-31
Preprint. Discussion started: 29 August 2023

Annex 5. Trends of the 99th percentile (P99) of significant wave height (SWH) over the Alborán Sea for the 1993-2022 period as derived from the regional wave reanalysis -product ref. no. 5 (Table 1)-. Areas with statistically significant trends at the 90% confidence intervals are denoted by black dots.